MOLECULAR AND CELLULAR BIOLOGY, July 2004, p. 6362–6378 Vol. 24, No. 14
0270-7306/04/$08.00+0 DOI: 10.1128/MCB.24.14.6362–6378.2004

The NEF4 Complex Regulates Rad4 Levels and Utilizes Snf2/Swi2-Related ATPase Activity for Nucleotide Excision Repair

Kerrington L. Ramsey, Joshua J. Smith, Arindam Dasgupta, Nazif Maqani, Patrick Grant, and David T. Auble*

Department of Biochemistry and Molecular Genetics, University of Virginia Health System, Charlottesville, Virginia 22908-0733

Received 23 March 2004/Accepted 20 April 2004

Nucleotide excision repair factor 4 (NEF4) is required for repair of nontranscribed DNA in *Saccharomyces cerevisiae*. Rad7 and the Snf2/Swi2-related ATPase Rad16 are NEF4 subunits. We report previously unrecognized similarity between Rad7 and F-box proteins. Rad16 contains a RING domain embedded within its ATPase domain, and the presence of these motifs in NEF4 suggested that NEF4 functions as both an ATPase and an E3 ubiquitin ligase. Mutational analysis provides strong support for this model. The Rad16 ATPase is important for NEF4 function in vivo, and genetic analysis uncovered new interactions between NEF4 and Rad23, a repair factor that links repair to proteasome function. Elc1 is the yeast homologue of a mammalian E3 subunit, and it is a novel component of NEF4. Moreover, the E2s Ubc9 and Ubc13 were linked to the NEF4 repair pathway by genetic criteria. Mutations in NEF4 or Ubc13 result in elevated levels of the DNA damage recognition protein Rad4 and an increase in ubiquitylated species of Rad23. As Rad23 also controls Rad4 levels, these results suggest a complex system for globally regulating repair activity in vivo by controlling turnover of Rad4.

UV light induces primarily the formation of cyclobutane pyrimidine dimers and (6-4) photoproducts in DNA (14). Nucleotide excision repair (NER) is the main pathway for removal of these lesions as well as for removal of a variety of other bulky DNA adducts (12, 14). All of the core components of the NER machinery have been identified and cloned, and the repair reaction has been reconstituted in vitro with highly purified or recombinant components (1, 19). The enzymatic activities (e.g., ATPase and structure-specific nuclease) and DNA binding properties of many proteins have been extensively described (2, 12). Multiple pairwise interactions between these components have also been detected (12, 19, 21), and based on these interactions, the *Saccharomyces cerevisiae* NER components can be subdivided into four nucleotide excision repair factors, NEF 1, 2, 3, and 4 (reviewed in reference 2).

While impressive progress has been made in defining the mechanism of the NER reaction in vitro, comparatively little is known about how the NER machinery contends with chromatin or how the repair reaction is regulated (17, 66, 71). Rad23, a nonessential NER component, participates in DNA damage recognition, physically links the proteasome to ubiquitylated substrates, and regulates ubiquitin chain elongation (2, 6, 9, 19, 57). These observations suggest that Rad23 performs a regulatory function in NER (66). In addition to Rad23, loss of Rad16 or Rad7 also gives rise to a moderate degree of UV sensitivity (5, 14, 48). These components have also been proposed to regulate the repair reaction or to augment repair of certain regions of the genome (51).

Rad16 and Rad7 form a stable complex called NEF4 (21) and are required in vivo for repair of transcriptionally silent DNA (e.g., *HMLα*) and repair of the nontranscribed strand of transcribed genes (5, 45, 67, 73). Overall, it has been estimated that Rad7 and Rad16 contribute to the repair of a substantial fraction of the genome: between 20 and 50% of UV-induced lesions in DNA require Rad7 and Rad16 for repair in vivo (73). Furthermore, transcription-coupled repair and Rad16-mediated global genome repair are the only NER pathways for handling DNA damage in the yeast *GAL* genes (40). Consistent with the roles of these proteins in repair of nontranscribed DNA, extracts made from cells with deletions of *RAD7* or *RAD16* are defective in transcription-independent repair in vitro (23, 76). The specific function(s) of Rad7 and Rad16 is unclear, however.

The Rad7 subunit of NEF4 interacts with the Rad4-Rad23 complex (called NEF2) via its Rad4 subunit (51, 76). NEF2 is involved directly in the recognition of DNA damage, and it functions to recruit other repair factors to sites of DNA damage (6). Rad16, a member of the Snf2/Swi2 ATPase family (13, 52), has DNA-stimulated ATPase activity, and it has been proposed that NEF4 functions as an ATP-driven motor which can scan along DNA to locate DNA damage (21). A number of DNA-stimulated ATPases in this protein family have been shown to remodel chromatin (74), leading to the suggestion that NEF4 might also function to open damaged chromatin, thereby allowing access by the NER machinery (51, 68). Rad16 also contains a zinc-binding domain called a RING-H2 finger (henceforth referred to as RING) (13, 52, 58). RING proteins can interact with ubiquitin-conjugating enzymes (Ubcs or E2s),

* Corresponding author. Mailing address: Department of Biochemistry and Molecular Genetics, University of Virginia Health System, 1300 Jefferson Park Ave., Room 6213, Charlottesville, VA 22908-0733. Phone: (434) 243-2629. Fax: (434) 924-5069. E-mail: dta4n@virginia.edu.

TABLE 1. Plasmids used in this study

Plasmid	Characteristics	Source
pRAD16-4	*GAL1-EE-RAD16 LEU2* 2μm	This study
pRAD16-11	*GAL1-EE-RAD16-K216A LEU2* 2μm	This study
pRAD16-16	*EE-RAD16 LEU2*	This study
pRAD16-17	*EE-RAD16-K216A LEU2*	This study
pRAD16-24	*EE-RAD16-C540A LEU2*	This study
pRAD16-25	*EE-RAD16-C557A LEU2*	This study
pRAD16-31	pET16b::*RAD16*	This study
pRAD16-35-3	pET16b::*RAD16,ELC1*	This study
pRAD16-500	*EE-RAD16-K216A,C540A LEU2*	This study
pRAD16-502	*EE-RAD16-C537A LEU2*	This study
pRAD16-503	*EE-RAD16-C580A LEU2*	This study
pRAD16-504	*EE-RAD16-C540A,C580A LEU2*	This study
pRAD16-507	*EE-RAD16-Y564A LEU2*	This study
pRAD16-508	*EE-RAD16-C560A LEU2*	This study
pRAD16-509	*EE-RAD16-K216A,Y564A LEU2*	This study
pAD6	pET41a::*RAD7*	This study
pAD15	*RAD7 TRP1*	This study
pAD16	*FLAG-RAD7 TRP1*	This study
pRAD7-500	*FLAG-RAD7-I37A TRP1*	This study
pRAD7-501	*FLAG-RAD-W41A TRP1*	This study
pRAD7-502	*FLAG-RAD7-K40A,Q43A TRP1*	This study
pRAD7-503	*FLAG-RAD7-ΔF-box TRP1*	This study
pET15b-ELC1	pET15b::*ELC1*	C. Koth
pELC1-500	*ELC1 HIS3*	This study
pELC1-501	*ELC1 LEU2*	This study
pELC1-502	*ELC1 URA3*	This study
pELC1-503	*HA-ELC1 HIS3*	This study
pELC1-504	*HA-ELC1 LEU2*	This study
pMT2104	*CUP1-GST-ELC1 URA3 leu2-d* 2μm	M. Tyers

and many function as ubiquitin-protein ligases (E3s) (3, 34, 44). E3s participate in an enzyme cascade in which ubiquitin (or a ubiquitin-like protein) is transferred from an E2 to a substrate protein (26).

We report that Rad7 has previously unrecognized similarity to the F-box subunits of SCF-type ubiquitin ligases, and we also define the yeast homologue of human elongin C Elc1, as a new component of NEF4. All three NEF4 subunits bear sequence hallmarks of ubiquitin ligase subunits. We demonstrate that the ATPase activity of NEF4 is important for its repair function in vivo, and mutational analysis demonstrates that NEF4 participates in a repair pathway that controls the steady-state levels of Rad4. The apparent ubiquitin ligase activity of NEF4 is phenotypically redundant with the activity of Rad23, and both of these factors control the steady-state level of Rad4, a ubiquitylated protein in *S. cerevisiae* (42). Rad23 is also known to be ubiquitylated (39). The results presented here better define the function of NEF4 and illuminate new complexity in NER involving posttranslational modification of Rad4 and Rad23. The modulation of Rad4 levels by NEF4 complements and extends recent observations indicating that the levels of a mammalian homologue of Rad4, XPC are likewise controlled by a ubiquitin-mediated pathway in mammalian cells (46), suggesting that the control of Rad4 levels is of fundamental importance in eukaryotes.

MATERIALS AND METHODS

Plasmids and yeast strains. The plasmids used in this study are described in Table 1. *CEN ARS* plasmids encoding *RAD16*, *RAD7*, and *ELC1* were constructed by PCR and standard subcloning procedures. The *RAD16* wild-type and mutant genes encode N-terminal polyomavirus medium T (Py) epitope tags recognizing the EE peptide (61), wild-type and mutant *RAD7* genes encode N-terminal Flag tags, and *ELC1* encodes a single N-terminal hemagglutinin (HA) epitope tag. Plasmids with the *RAD16* gene were obtained by subcloning from pBLTY4 (60). The *RAD7* constructs were obtained by subcloning the *RAD7* open reading frame (ORF) from pDG649 (47), and the *RAD7* promoter was obtained by PCR of yeast genomic DNA. The *ELC1* ORF plus 300 bp of 5′ and 3′ flanking DNA was PCR amplified from genomic DNA and subcloned into pRS413 (pELC1-500) (65). The *HA-ELC1* plasmid was obtained by subcloning a ClaI- and BamHI-cut fragment containing the *HA-ELC1* ORF from pYeF1H-*ELC1* (a gift from Linda Hyman) (32) into pELC1-500 cut with ClaI and BamHI.

pET15b-ELC1 was obtained from Chris Koth (38). pAD6 was made by inserting an EcoRI fragment from pDG649 (containing the entire *RAD7* ORF) into the EcoRI site of pET41a (Novagen). pRAD16-31 was obtained by inserting the Py-tagged *RAD16* ORF into the NdeI and BamHI sites of pET16b (Novagen). pRAD16-35-3 is derived from pET16b and was used for expression of both Py-tagged Rad16 and Elc1 under T7 control, both with histidine tags. Site-directed mutations were generated by overlapping PCR (4) or with the Stratagene Quick Change kit as recommended by the manufacturer. pMT2104 (25) expresses glutathione *S*-transferase (*GST*)–*ELC1* under *CUP1* control and was a gift from Mike Tyers. Additional details concerning plasmid construction are available upon request.

The strains used in this study are described in Table 2. *RAD16* was deleted by one-step transformation with pBLY22 (60), obtained from Brehon Laurent. Other gene deletions were constructed as previously described (16, 43) with PCR-generated *HIS3*, *KANMX*, or *NATMX* cassettes for yeast transformation. Tandem affinity purification (TAP)-tagged strains were generated by integration of sequences encoding the TAP tag immediately 3′ of the indicated ORF (54). Appropriate integration events were confirmed by PCR.

UV survival assays. Cells were grown in liquid culture (YPD or the appropriate dropout medium for plasmid selection) to an optical density at 600 nm of about 1.0 at 30°C unless otherwise indicated. Following mild sonication to disperse clumps of cells, the cells were plated on YPD or the appropriate dropout agar and irradiated in a Stratalinker with the indicated doses of UV light. The UV dose delivered was calculated with a UVX radiometer (UVP). Following irradiation, plates were immediately wrapped in foil and incubated for 2 to 4 days at 30°C (or the indicated temperature). Cell survival was determined from the number of colonies relative to that in the unirradiated control. Experiments were performed in triplicate, and the error bars on the graphs represent standard deviations.

Alternatively, *S. cerevisiae* strains were analyzed for UV sensitivity by UV irradiation of spot dilutions of the indicated strains. For spot assays, strains were grown at 30°C (unless otherwise indicated) to an optical density at 600 nm of 1.0 and washed in sterile water, and 10-fold serial dilutions were spotted on YPD or appropriate dropout plates. Once dried, the plates were UV irradiated as indicated above. Experiments were performed in triplicate with different clones, and sensitivity to UV was graded according to the point at which growth was inhibited.

ATPase activity assays. Expression and purification of Py epitope-tagged Rad16 used for the ATPase assays was similar to the procedure described previously (4) with the following modifications. For high-copy-number expression of *RAD16* or *RAD16-K216A* under *GAL1* control, strains were grown in 5-ml cultures of yeast extract-peptone medium with 2% raffinose and then subcultured into 100 ml of synthetic medium plus raffinose but lacking leucine. A strain bearing pRS425 was used for the plasmid vector control. When the cells had reached an approximate optical density at 600 nm of 1.0, protein expression was induced by addition of galactose to 2% for 2 h at 30°C. Cells were harvested by centrifugation and washed in 10 ml of extraction buffer (200 mM Tris-HCl [pH 8.0], 400 mM ammonium sulfate, 10 mM magnesium chloride, 1 mM EDTA, 10% glycerol, 7 mM β-mercaptoethanol, 1.0 mM phenylmethylsulfonyl fluoride, 2.0 mM benzamidine, 2.0 μM pepstatin, 0.6 μM leupeptin, and 2.0 μg of chymostatin per ml). The cell pellets were then resuspended in 400 μl of extraction buffer, and glass beads (400 to 625 μm in diameter) were used to disrupt cells by vortexing, and large debris and unlysed cells were removed from the lysate by centrifugation. Protein concentrations were determined by the Bradford assay with bovine serum albumin as the standard. Extracts were stored at −80°C.

Purification of epitope-tagged Rad16 from yeast whole-cell extracts was performed by incubation of 1.0 mg of extract protein with 60 μl of Py antibody-coupled beads in 300 μl of HEG buffer (20 mM HEPES [pH 7.6 with KOH], 1 mM EDTA, 10% glycerol, 1 mM dithiothreitol, and protease inhibitors as described above) plus 300 mM potassium acetate and 0.1% octylglucoside. The extracts were incubated with the beads for 2 h at 4°C with rotation. Beads were then washed four times with 1 ml of HEG buffer plus 0.5 M potassium acetate and 0.1% Nonidet P-40 and once with 1 ml of HEG plus 0.2 M potassium acetate

TABLE 2. Strains used in this study

Strain	Genotype	Reference or source
YPH499	*MAT***a** *ura3-52 lys3-52 lys2-801^a ade2-101^o trp1-Δ63 his3-Δ200 leu2-Δ1*	65
YPH500	*MATα ura3-52 lys3-52 lys2-801^a ade2-101^o trp1-Δ63 his3-Δ200 leu2-Δ1*	65
AY68	*MATα ura3-52 lys3-52 lys2-801^a ade2-101^o trp1-Δ63 his3-Δ200 leu2-Δ1 rad16Δ::URA3*	This study
KLR1	*MATα ura3-52 lys3-52 lys2-801^a ade2-101^o trp1-Δ63 his3-Δ200 leu2-Δ1 rad7Δ::KAN*	This study
KLR2	*MAT***a** *ura3-52 lys3-52 lys2-801^a ade2-101^o trp1-Δ63 his3-Δ200 leu2-Δ1 rad23Δ::HIS3*	This study
KLR3	*MATα ura3-52 lys3-52 lys2-801^a ade2-101^o trp1-Δ63 his3-Δ200 leu2-Δ1 rad7Δ::KAN rad23Δ::HIS3*	This study
KLR4	*MATα ura3-52 lys3-52 lys2-801^a ade2-101^o trp1-Δ63 his3-Δ200 leu2-Δ1 rad7Δ::KAN rad16Δ::URA3 rad23Δ::HIS3*	This study
KLR5	*MATα ura3-52 lys3-52 lys2-801^a ade2-101^o trp1-Δ63 his3-Δ200 leu2-Δ1 rad7Δ::KAN rad16Δ::URA3*	This study
KLR6	*MAT***a** *ura3-52 lys3-52 lys2-801^a ade2-101^o trp1-Δ63 his3-Δ200 leu2-Δ1 elc1Δ::NAT*	This study
KLR7	*MATα ura3-52 lys3-52 lys2-801^a ade2-101^o trp1-Δ63 his3-Δ200 leu2-Δ1 rad7Δ::KAN elc1Δ::NAT*	This study
KLR8	*MAT***a** *ura3-52 lys3-52 lys2-801^a ade2-101^o trp1-Δ63 his 3-Δ200 leu2-Δ1 rad23Δ::HIS3 elc1Δ::NAT rad7Δ::KAN*	This study
KLR14	*MATα ura3-52 lys3-52 lys2-801^a ade2-101^o trp1-Δ63 his 3-Δ200 leu2-Δ1 RAD4TAP-URA3 rad7Δ::KAN rad23Δ::HIS3*	This study
KLR15	*MATα ura3-52 lys3-52 lys2-801^a ade2-101^o trp1-Δ63 his 3-Δ200 leu2-Δ1 RAD4TAP-URA3 rad7Δ::KAN*	This study
JJSY283	*MATα ura3-52 lys3-52 lys2-801^a ade2-101^o trp1-Δ63 his 3-Δ200 leu2-Δ1 RAD4TAP-URA3 elc1Δ::NAT*	This study
JJSY284	*MAT***a** *ura3-52 his 3-Δ200 leu2-Δ1 RAD4TAP-URA3 ubc13Δ::KAN*	This study
JJSY285	*MAT***a** *ura3-52 trp1-Δ63his 3-Δ200 leu2-Δ1 ubc9Δ::TRP ubc9-1::LEU2::LEU2 RAD4TAP-URA3*	This study
JJSY297	*MATα ura3-52 lys3-52 lys2-801^a ade2-101^o trp1-Δ63 his 3-Δ200 leu2-Δ1 RAD4TAP-URA3 rad16Δ::URA3*	This study
JJSY505	*MATα ura3Δ0 leu2Δ0 his 3Δ1 met15Δ0 RAD4TAP-URA3 cim5^{ts}*	This study
JJSY506	*MATα ura3Δ0 leu2Δ0 his 3Δ1 met15Δ0 RAD4TAP-URA3 cim5^{ts} rad7Δ::KAN*	This study
KLR16	*MAT***a** *his3Δ1 leu2Δ met15Δ ura3Δ RAD7TAP-URA3*	This study
KLR17	*MAT***a** *his3Δ1 leu2Δ met15Δ ura3Δ RAD7TAP-URA3 rad16Δ::KAN*	This study
KLR18	*MAT***a** *his3Δ1 leu2Δ met15Δ ura3Δ RAD7TAP-URA3 rad16Δ::KAN elc1Δ::NAT*	This study
KLR19	*MAT***a** *his3Δ1 leu2Δ met15Δ ura3Δ RAD16TAP-URA3*	This study
KLR20	*MAT***a** *his3Δ1 leu2Δ met15Δ ura3Δ RAD16TAP-URA3 rad7Δ::KAN*	This study
KLR21	*MATα ura3-52 lys3-52 lys2-801^a ade2-101^o trp1-Δ63 his 3-Δ200 leu2-Δ1 RAD16TAP-URA3 rad7Δ::KAN elc1Δ::NAT*	This study
KLR22	*MATα ura3-52 lys3-52 lys2-801^a ade2-101^o trp1-Δ63 his 3-Δ200 leu2-Δ1 rad16Δ::URA3 ubc4Δ::KAN*	This study
KLR23	*MAT***a** *ura3-52 lys3-52 lys2-801^a ade2-101^o trp1-Δ63 his 3-Δ200 leu2-Δ1 ubc4Δ::KAN*	This study
KLR24	*MATα ura3-52 lys3-52 lys2-801^a ade2-101^o trp1-Δ63 his 3-Δ200 leu2-Δ1 rad16Δ::URA3 ubc5Δ::HIS3*	This study
KLR25	*MAT***a** *ura3-52 lys3-52 lys2-801^a ade2-101^o trp1-Δ63 his 3-Δ200 leu2-Δ1 ubc5Δ::HIS3*	This study
BY4741	*MAT***a** *his3Δ1 leu2Δ met15Δ ura3Δ*	M. Smith
BY4742	*MATα his3Δ1 leu2Δ lys2Δ ura3Δ*	M. Smith
JJSY13	*MATα his3Δ1 leu2Δ lys2Δ ura3Δ rad23Δ::NAT*	This study
ubc2Δ	*MAT***a** *his3Δ1 leu2Δ met15Δ ura3Δ ubc2Δ::KAN*	EUROSCARF
ubc4Δ	*MAT***a** *his3Δ1 leu2Δ met15Δ ura3Δ ubc4Δ::KAN*	EUROSCARF
ubc5Δ	*MAT***a** *his3Δ1 leu2Δ met15Δ ura3Δ ubc5Δ::KAN*	EUROSCARF
ubc7Δ	*MAT***a** *his3Δ1 leu2Δ met15Δ ura3Δ ubc7Δ::KAN*	EUROSCARF
ubc8Δ	*MAT***a** *his3Δ1 leu2Δ met15Δ ura3Δ ubc8Δ::KAN*	EUROSCARF
ubc10Δ	*MAT***a** *his3Δ1 leu2Δ met15Δ ura3Δ ubc10Δ::KAN*	EUROSCARF
ubc11Δ	*MAT***a** *his3Δ1 leu2Δ met15Δ ura3Δ ubc11Δ::KAN*	EUROSCARF
ubc12Δ	*MAT***a** *his3Δ1 leu2Δ met15Δ ura3Δ ubc12Δ::KAN*	EUROSCARF
ubc13Δ	*MAT***a** *his3Δ1 leu2Δ met15Δ ura3Δ ubc13Δ::KAN*	EUROSCARF
rad16Δ	*MAT***a** *his3Δ1 leu2Δ met15Δ ura3Δ rad16Δ::KAN*	EUROSCARF
JJSY58	*MAT***a** *his3Δ1 leu2Δ met15Δ ura3Δ ubc2Δ::KAN rad23Δ::NAT*	This study
JJSY61	*MAT***a** *his3Δ1 leu2Δ met15Δ ura3Δ ubc4Δ::KAN rad23Δ::NAT*	This study
JJSY65	*MATα his3Δ1 leu2Δ lys2Δ ura3Δ ubc5Δ::KAN rad23Δ::NAT*	This study
JJSY68	*MAT***a** *his3Δ1 leu2Δ met15Δ ura3Δ ubc7Δ::KAN rad23Δ::NAT*	This study
JJSY70	*MAT***a** *his3Δ1 leu2Δ met15Δ ura3Δ ubc8Δ::KAN rad23Δ::NAT*	This study
JJSY72	*MAT***a** *his3Δ1 leu2Δ met15Δ ura3Δ ubc10Δ::KAN rad23Δ::NAT*	This study
JJSY74	*MAT***a** *his3Δ1 leu2Δ met15Δ ura3Δ ubc12Δ::KAN rad23Δ::NAT*	This study
JJSY78	*MAT***a** *his3Δ1 leu2Δ met15Δ ura3Δ ubc13Δ::KAN rad23Δ::NAT*	This study
MHY501	*MATα his3Δ-200 leu2-3,112 ura3-52 lys2-801 trp1-1*	M. Hochstrasser
MSY1211	*MAT***a** *his3Δ leu2Δ lys2Δ trp1Δ ura3Δ*	M. Smith
MHY509	*MATα his3Δ-200 leu2-3,112 ura3-52 lys2-801 trp1-1 ubc1Δ::HIS3*	M. Hochstrasser
MHY495	*MATαhis3Δ-200 leu2-3,112 ura3-52 lys2-801 trp1-1 ubc6Δ::HIS3*	M. Hochstrasser
JJSY103	*MATα his3Δ-200 leu2-3, 112 ura3-52 lys2-801 trp1-1 ubc6Δ::HIS3 rad23Δ::NAT*	This study
MSY1212	*MAT***a** *his3Δ leu2Δ lys2Δ trp1Δ ura3Δ ubc9Δ::TRP ubc9-1::LEU2::LEU2*	M. Smith
JJSY106	*MAT***a** *his3Δ1 leu2Δ met15Δ ura3Δ ubc11Δ::KAN rad23Δ::NAT*	This study
MSY347	*MAT***a** *cdc34 his3Δ ura3-52*	M. Smith
JJSY118	*MAT***a** *his3Δ leu2Δ lys2Δ trp1Δ ura3Δ rad23Δ::NAT*	This study
JJSY122	*MATα his3Δ-200 leu2-3,112 ura3-52 lys2-801 trp1-1 rad23Δ::NAT*	This study

Continued on following page

TABLE 2—*Continued*

Strain	Genotype	Reference or source
JJSY123	*MAT***a** *leu2-2 ura3-1 trp1-1his3-11 his15 ade2-1can1-100 rad23*Δ*::NAT*	This study
JJSY124	*MAT*α *his3*Δ*-200 leu2-3,112 ura3-52 lys2-801 trp1-1 ubc1*Δ*::HIS3 rad23*Δ*::NAT*	This study
JJSY125	*MAT***a** *his3*Δ *leu2*Δ *lys2*Δ *trp1*Δ *ura3*Δ *ubc9*Δ*::TRP ubc9-1::LEU2::LEU2 rad23*Δ*::NAT*	This study
JJSY151	*MAT***a** *his3*Δ*1 leu2*Δ *lys2*Δ *ura3*Δ *ubc13*Δ*::KAN rad23*Δ*::NAT rad16*Δ*::URA3*	This study
JJSY152	*MAT***a** *his3*Δ*1 leu2*Δ *lys2*Δ *ura3*Δ *ubc2*Δ*::KAN rad23*Δ*::NAT rad16*Δ*::URA3*	This study
JJSY156	*MAT***a** *his3*Δ *leu2*Δ *lys2*Δ *trp1*Δ *ura3*Δ *rad16*Δ*::URA3*	This study
JJSY159	*MAT***a** *his3*Δ*-200 leu2-3,112 ura3-52 lys2-801 trp1-1 rad16*Δ*::URA3*	This study
JJSY162	*MAT*α *his3*Δ*1 leu2*Δ *lys2*Δ *ura3*Δ *rad23*Δ*::NAT rad16*Δ*::URA3*	This study
JJSY163	*MAT***a** *his3*Δ *leu2*Δ *lys2*Δ *trp1*Δ *ura3*Δ *ubc9*Δ*::TRP ubc9-1::LEU2 rad16*Δ*::URA3*	This study
JJSY165	*MAT***a** *his3*Δ*1 leu2*Δ *met15*Δ *ura3*Δ *ubc13*Δ*::KAN rad16*Δ*::URA3*	This study
JJSY167	*MAT***a** *his3*Δ*1 leu2*Δ *met15*Δ *ura3*Δ *ubc2*Δ*::KAN rad16*Δ*::URA3*	This study
JJSY171	*MAT***a** *cdc34 his3*Δ *ura3-52 rad16*Δ*::URA3*	This study
JJSY174	*MAT*α *his3*Δ*-200 leu2-3,112 ura3-52 lys2-801 trp1-1 ubc1*Δ*::HIS3 rad16*Δ*::URA3*	This study
JJSY191	*MAT***a** *cdc34 his3*Δ *ura3-52 rad23*Δ*::NAT*	This study
JJSY238	*MAT***a** *his3*Δ*1 leu2*Δ *met15*Δ *ura3*Δ *ubc8*Δ*::KAN rad16*Δ*::URA3*	This study
JJSY240	*MAT***a** *his3*Δ *leu2*Δ *lys2*Δ *trp1*Δ *ura3*Δ *rad23*Δ*::NAT rad16*Δ*::URA3*	This study
JJSY242	*MAT***a** *his3*Δ*1 leu2*Δ *met15*Δ *ura3*Δ *ubc8*Δ*::KAN rad23*Δ*::NAT rad16*Δ*::URA3*	This study
JJSY243	*MAT***a** *his3*Δ *leu2*Δ *lys2*Δ *trp1*Δ *ura3*Δ *ubc9*Δ*::TRP ubc9-1::LEU2::LEU2 rad23*Δ*::NAT rad16*Δ*::URA3*	This study
YJG1	*MAT***a** *ura3*Δ*0 met15*Δ*0 trp1-*Δ*63 his3-*Δ*200 TAPRAD23-TRP1*	This study
JJSY358	*MAT***a** *ura3*Δ*0 met15*Δ*0 trp1-*Δ*63 his3-*Δ*200 TAPRAD23-TRP1 rad16*Δ*::URA3*	This study
JJSY360	*MAT***a** *ura3*Δ*0 met15*Δ*0 trp1-*Δ*63 his3-*Δ*200 TAPRAD23-TRP1 rad7*Δ*::KAN*	This study
JJSY362	*MAT***a** *ura3*Δ*0 met15*Δ*0 trp1-*Δ*63 his3-*Δ*200 TAPRAD23-TRP1 ubc13*Δ*::KAN*	This study
JJSY367	*MAT***a** *ura3*Δ*0 met15*Δ*0 trp1-*Δ*63 his3-*Δ*200 TAPRAD23-TRP1 ubc2*Δ*::KAN*	This study

and 0.1% Brij 58. Bound protein was eluted in two 50-μl washes of HEG plus 0.2 M potassium acetate and 0.1% Brij 58 containing 0.2 mg of Py-peptide per ml following incubation at room temperature for 10 min each. Purified protein yields were determined both by Western blotting with the Py monoclonal antibody and by Coomassie staining polyacrylamide gels with known amounts of bovine serum albumin for quantitation. The affinity-purified protein was stored at −80°C.

Approximately 40 ng of purified Rad16, Rad16-K216A, or mock-purified material was mixed with 250 ng of ϕX double-stranded DNA in a 20-μl reaction mixture containing 10 μM unlabeled ATP and 1 μCi of [γ^{32}P]ATP (6,000 Ci/mmol; Perkin Elmer) in buffer B (30 mM Tris-HCl [pH 7.5], 5 mM $MgCl_2$, 1 mM dithiothreitol, 100 μg of bovine serum albumin). The reaction mixtures were incubated for various times at room temperature, and the reactions were terminated by adding 1 μl of 100 mM EDTA plus 1 μl of 12 mM ATP to each reaction mix. One microliter was then spotted onto BakerFlex polyethyleneimine thin-layer chromatography plates, which were developed in 0.6 M KH_2PO_4 (pH 3.4). The plates were air dried, and the amount of hydrolyzed ATP was quantified by analysis with a Molecular Dynamics PhosphorImager.

Extract preparation and Western blotting. Whole-cell extracts were prepared with glass beads by either manually vortexing or use of a Fast Prep machine (Bio 101) as recommended by the manufacturer. For the extracts in Fig. 6 and 9, cells were lysed in 20 mM Tris-acetate (pH 8.0), 300 mM potassium acetate, 20% glycerol, 5 mM β-mercaptoethanol, 1 mM phenylmethylsulfonyl fluoride, 0.3 μg of leupeptin per ml, and 1.4 μg of pepstatin per ml. For the extracts in Fig. 2, 3, and 4, cells were lysed in 40 mM HEPES (pH 7.5), 350 mM NaCl, 1% Triton X-100, 10% glycerol, 1 mM dithiothreitol, 1 mM phenylmethylsulfonyl fluoride, 0.3 μg of leupeptin per ml, and 1.4 μg of pepstatin per ml.

To determine the levels of Rad4, *S. cerevisiae* strains were grown as for the UV survival assays, and cells were washed in sterile water, treated with UV light at 100 J/m^2, and allowed to recover in fresh medium for 2 h in foil-wrapped flasks. Samples were taken at the indicated times following UV treatment, and whole-cell extracts were prepared. For induction of GST-Elc1, cells were induced by addition of copper sulfate to 0.5 mM, and cells were harvested after 1 h of induction. Protein yields were determined with the Bradford protein assay (Bio-Rad); equivalent amounts of whole-cell extract protein were resolved on polyacrylamide protein gels and transferred to Immobilon-P (Millipore). Membranes were blocked in 5% nonfat dry milk in 50 mM Tris-Cl (pH 7.5), 0.9% NaCl, 0.05% Tween 20, and 0.01% antifoam A, and proteins were detected with antibodies at the following dilutions: M2 Flag (Sigma), 1:5,000; Py monoclonal, 1:200; 12CA5 anti-HA monoclonal, 1:3,000; anti-protein A, 1:50,000; and anti-GST (Amersham), 1:12,500. Anti-mouse and anti-rabbit immunoglobulin secondary antibodies (Amersham) were used at 1:5,000, and anti-goat immunoglobulin antibody was used at 1:10,000. Proteins were detected with the Amersham ECL+ kit as recommended by the manufacturer. All rad16 and rad7 mutant proteins listed in Table 3 were expressed at levels that were similar to the wild-type levels, as determined by Western blotting analysis (not shown). Bacterially expressed proteins were detected with either anti-GST antibody at 1:5,000 and secondary anti-goat antibody at 1:10,000; anti-His antibody (Santa Cruz Biotechnology) at 1:2,000 and anti-rabbit secondary antibody at 1:2,000; or Py monoclonal antibody at 1:5,000 with anti-mouse secondary antibody at 1:5,000.

Coimmunoprecipitation experiments. Three to five milligrams of yeast whole-cell extract protein was incubated with 20 to 40 μl of HA antibody-coupled agarose beads (Roche), Flag M2 antibody-coupled beads (Sigma), calmodulin affinity resin (Stratagene), or immunoglobulin G-Sepharose 6 fast flow (Amersham) in cell lysis buffer (see above). Immunoprecipitation with calmodulin beads was performed in buffer that also contained 2 mM $CaCl_2$. Extracts were incubated with the beads at 4°C for 3 h with gentle mixing. Bead-bound complexes were washed three times at 4°C with 1 to 2 ml of the same buffer; the beads were then suspended in sodium dodecyl sulfate sample buffer, boiled, and loaded on gels.

Bacterial expression of Rad7, Rad16, and Elc1. BL-21 codon-positive cells harboring the indicated expression plasmids were inoculated into 6 ml of YT medium (0.55% yeast extract, 0.83% NaCl, and 1.33% tryptone) with appropriate drug selection (ampicillin and/or kanamycin) at 37°C with shaking for 6 h. The cultures were then added to 1 liter of selective medium and incubated at 18°C with shaking until the optical density at 600 nm reached approximately 0.6 to 1.0. Expression was induced by addition of isopropyl-β-D-thiogalactoside to 1 mM, and cells were harvested after 2 h at 18°C. Cells were subjected to three cycles of freezing and thawing, resuspended in 137 mM NaCl–2.7 mM KCl–10 mM Na_2HPO_4–1.8 mM KH_2PO_4–10% glycerol–1 mM phenylmethylsulfonyl fluoride–31 μg of benzamidine per ml–1.4 μg of pepstatin per ml –0.2 μg of chymostatin per ml–0.3 μg of leupeptin per ml, and lysed by sonication. Cell lysates were clarified by centrifugation and incubated with glutathione-Sepharose 4B (Amersham Biosciences) for 2 h at 4°C. Unbound material was removed by washing the beads with lysis buffer, and bound and unbound material was analyzed by Western blotting as described above.

Sequence analysis. PSI-BLAST search (http://www.ncbi.nlm.nih.gov/BLAST/) of the SWISSPROT and *S. cerevisiae* databases was performed with the Rad7 sequence (accession number A25226) as the query with default settings. Grr1 (accession number NP_012623) was the only protein detected with a significant expectation value (E, $\approx 10^{-4}$). The significance of the alignment was confirmed by performing a similar analysis with shuffled sequences with PRSS (http://www.ch.embnet.org/software/PRSS_form.html). A BLOCKS search (http:

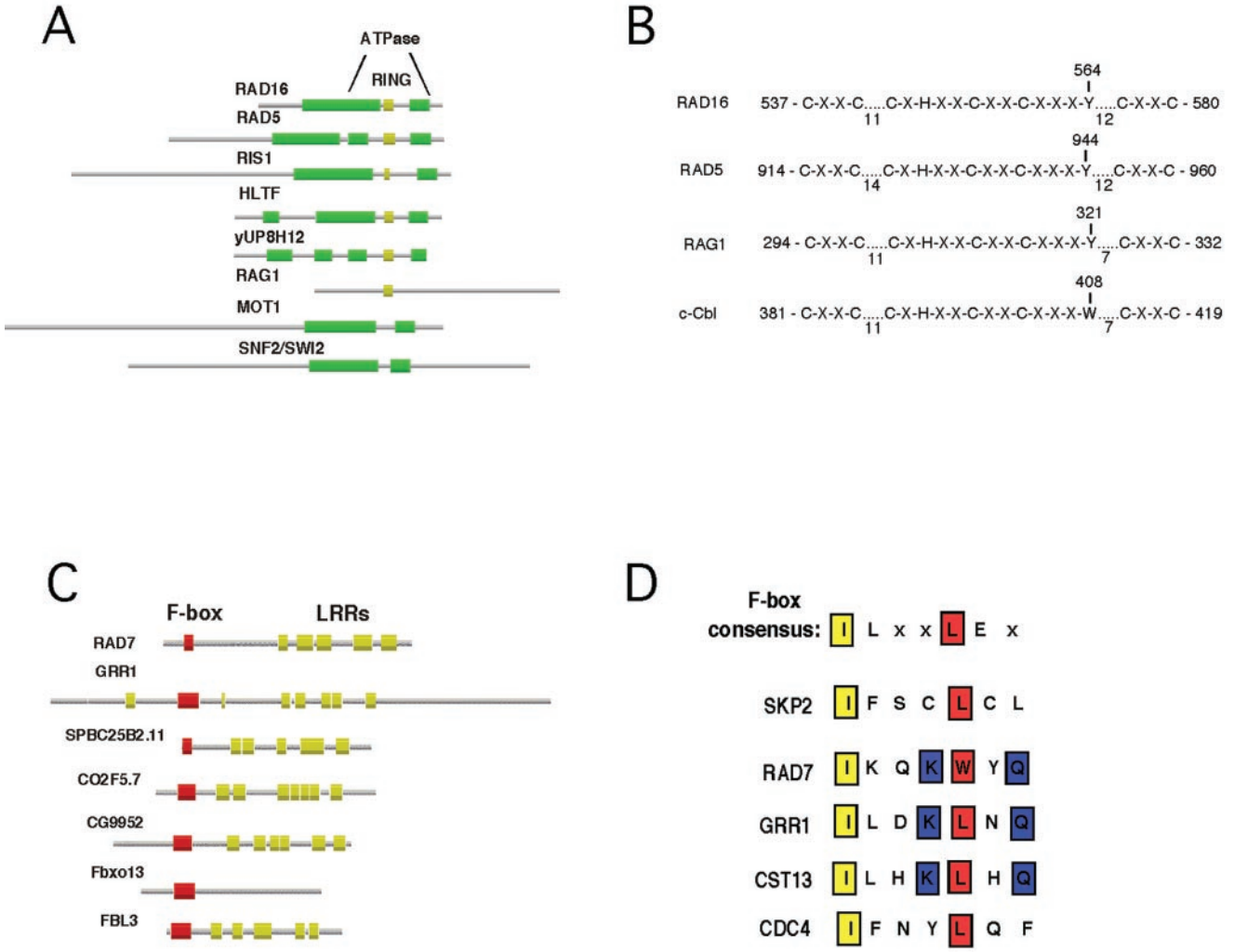

FIG. 1. Conserved sequences in Rad16 and Rad7. (A) Alignment of Rad16 with some of its homologous proteins containing Snf2/Swi2-related ATPase domains (green) and RING domains (yellow). (B) Alignment of the Rad16 RING domain with the RING domains of Rad5, RAG1, and c-Cbl. Note that Rad16 Y564 is analogous to c-Cbl W408 (81) and Rad5 Y944 (69), necessary for interaction of c-Cbl and Rad5 with their E2s. (C) Alignment of Rad7 with some of its homologous proteins containing F-box domains (red) and leucine-rich repeats (LRRs, yellow). (D) Alignment of F-box residues from different proteins; the F-box consensus sequence shown at the top. Rad7 residues in boxes were mutated in this study.

//blocks.fhcrc.org/blocks/blocks_search.html) identified the F-box domain in Rad7. The leucine-rich repeats in Rad7 were reported previously (62). Furthermore, when searching with Rad7 with SGD (http://www.yeastgenome.org/), BLAST searches show that the proteins listed in Fig. 1C were homologous to Rad7. The PSI-BLAST search engine was also used to search SWISSPROT with Rad16 (accession number NP_009672) as the query sequence. There were 201 hits on iteration 1 and Fig. 1 lists eight of these, including Rad16. The homologous proteins listed have expectation values (E) of less than 10^{-3}. Rad16's RING domain was reported previously (13, 52) and was also identified with the PFAM (http://www.sanger.ac.uk/Software/Pfam/search.shtml) and BLOCKS databases.

RESULTS

Sequence analysis of Rad16 and Rad7. As shown in Fig. 1A and B, Rad16 is a member of a subfamily of Snf2/Swi2-related proteins that contain RING domains inserted between blocks of conserved sequences that comprise the ATPase domain (5, 13, 52, 58). The general activity of RING domain proteins as E3s (34, 44) suggested an unanticipated role for Rad16 in a ubiquitin-mediated repair pathway. E3s function via physical interaction between the RING domain and an E2 (26, 81). The RING domains of Rag1 and Rad5 are homologous to the Rad16 RING domain (Fig. 1A and B), and both Rag1 and Rad5 have E3 activity or are components of multisubunit E3 complexes (69, 77). Thus, Rad16 is homologous to proteins with known E3 activity. These results suggest that the Rad16 RING domain physically interacts with an E2.

Substrates for ubiquitylation are recruited via specific interactions between the substrate and an E3 subunit, which is often distinct from the RING protein (26, 80, 81). We observed that the NEF4 subunit Rad7 bears striking similarity to substrate recognition subunits of SCF-like E3s. Rad7 was previously reported to contain 12 C-terminal leucine-rich repeats (62). As shown in Fig. 1C and D, the Rad7 N-terminal region has similarity to the N-terminal F-box domain of Grr1 and related

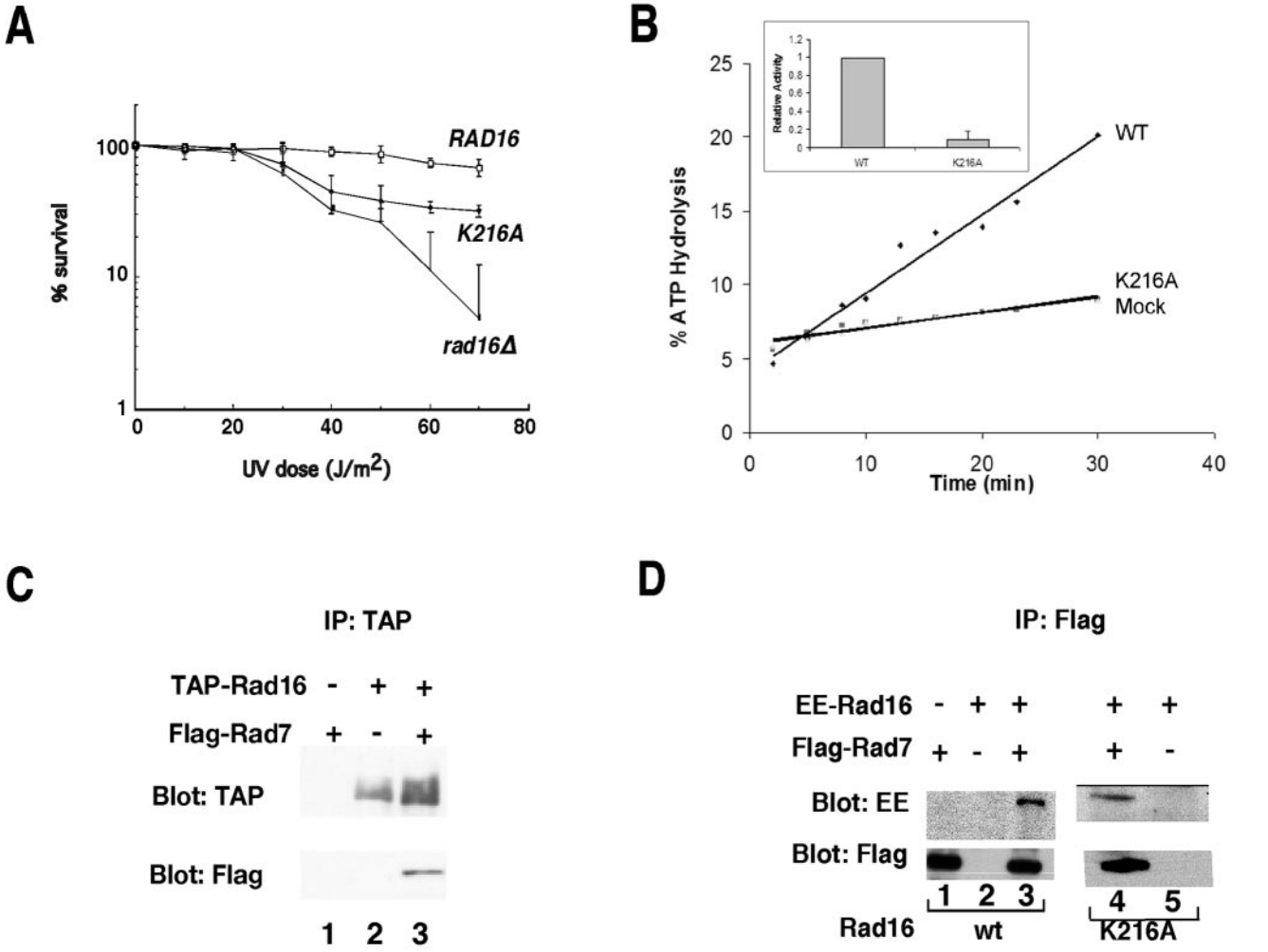

FIG. 2. Mutation of the ATPase domain impaired Rad16 function in vivo. (A) UV sensitivity of wild-type (*RAD16*), *rad16*Δ, and *rad16-K216A* strains. The graph shows the relative number of colonies that grew on agar plates following irradiation with the indicated doses of UV irradiation; 100% survival represents the number of colonies on the unirradiated control plates for each strain. For this and all subsequent graphs, the error bars represent the standard deviations determined from measurements made in triplicate. (B) ATP hydrolysis catalyzed by wild-type Rad16 (WT), rad16-K216A (K216A), or mock-purified material from cells with untagged Rad16 (Mock) was determined after incubation of reaction mixtures with the indicated proteins for the indicated times. The inset shows the relative ATPase activity of wild-type Rad16 and rad16-K216A derived from the hydrolysis detected following a 10-min incubation. The error bar represents the standard deviation derived from three separate experiments. Note that the very low ATPase activity of the rad16-K216A preparation was indistinguishable from that of the mock-purified material. (C) Co-immunoprecipitation of Flag-tagged Rad7 and TAP-tagged Rad16 in yeast whole-cell extracts. Extracts containing TAP-tagged Rad16 and/or Flag-tagged Rad7 (+) or untagged proteins (−) were immunoprecipitated with calmodulin beads, which bind the TAP tag on Rad16. Western blots of the immunoprecipitated material were probed for either Rad16 (protein A antibody) or Rad7 (Flag antibody). (D) Similar to panel C except that Flag-tagged Rad7 was immunoprecipitated with anti-Flag beads and the immunoprecipitates were probed with Flag antibody to detect Flag-Rad7 or Py monoclonal antibody to detect EE-tagged Rad16 (lanes 1 to 3) or rad16-K216A (lanes 4 and 5).

F-box proteins. The presence of a RING domain-containing subunit and an F-box-containing subunit in the NEF4 complex provides strong circumstantial support for the idea that the NEF4 complex functions as both an E3 and an ATPase.

Function of Rad16 RING domain and ATPase in vivo. To test the idea that NEF4 has dual functions in NER, mutations were made in the motifs identified above, and strains harboring these alleles were analyzed for UV sensitivity. In parallel, the effects of these mutations on NEF4 complex stability were determined by performing coimmunoprecipitation assays. First, the requirement for Rad16 ATPase activity was tested through mutation of lysine 216 to alanine. Lysine 216 is in the Walker A box (75) and is a conserved catalytic residue essential for ATPase activity of all Snf2/Swi2 ATPases that have been tested (49). As shown in Fig. 2A, the K216A mutation impaired Rad16 function in vivo, but rad16-K216A retained some activity, suggesting that it has some ATPase-independent function. To determine if the K216A mutation destroyed ATPase activity, ATPase assays were performed with affinity-purified wild-type Rad16, rad16-K216A, or material obtained from a mock purification with extract containing untagged Rad16. As shown in Fig. 2B, wild-type Rad16 had readily detectable ATPase activity, whereas the rad16-K216A mutant had no detectable ATPase activity. These results indicate that,

TABLE 3. Summary of Rad16 and Rad7 mutant data

Allele	UV sensitivity[a] in background:		Coimmunoprecipitation[b] in background:		Location of mutation
	RAD23$^+$	*rad23*Δ	*RAD23*$^+$	*rad23*Δ	
Rad16					
K216A	Intermediate	Intermediate	+		ATPase (Walker A)
C537A	Same as *rad16*Δ	Same as *rad16*Δ *rad23*Δ	−		RING domain
C540A	Intermediate	Same as *rad16*Δ *rad23*Δ	−		RING domain
C557A	Wild type	Same as *rad16*Δ *rad23*Δ	−		RING domain
C560A	Intermediate	Same as *rad16*Δ *rad23*Δ	−	−	RING domain
Y564A	Wild type	Same as *rad16*Δ *rad23*Δ	+	+	RING domain
C580A	Intermediate	Same as *rad16*Δ *rad23*Δ	−		RING domain
C540A,K216A	Same as *rad16*Δ	Same as *rad16*Δ *rad23*Δ	−		RING and Walker A
C540A,C580A	Same as *rad16*Δ	Same as *rad16*Δ *rad23*Δ	−		RING domain
Y564A,K216A	Intermediate	Same as *rad16*Δ *rad23*Δ	+	+	RING and Walker A
Rad7					
I37A	Wild type	Intermediate	+	+	F-box
W41A	Wild type	Same as *rad23*Δ			F-box
K40A,Q43A	Wild type	Intermediate	+	+	F-box
Δ37–43	Wild type	Same as *rad7*Δ *rad23*Δ	+	+	F-box deletion

[a] Intermediate, the strain is UV sensitive compared to the wild-type strain but not as UV sensitive as a strain with a deletion of the gene of interest; same as *rad16*Δ, the UV sensitivity of the strain carrying this allele is the same as the UV sensitivity of a strain with a deletion of the gene.
[b] +, Rad16 and Rad7 coimmunoprecipitate; −, the two proteins do not coassociate. If no result is shown, the combination was not tested.

indeed, rad16-K216A retains some other activity in vivo despite the fact that its ATPase activity has been abolished. Wild-type Rad16 and Rad7 were coimmunoprecipitated from cell extracts, and as expected, the K216A mutation did not detectably affect the association of Rad16 and Rad7 (Fig. 2C and D).

RING domains consist of conserved cysteine and histidine residues that coordinate two zinc atoms (Fig. 1B) (58); a conserved hydrophobic residue is also essential for interaction between RING domains and certain E2s (Fig. 1B) (81). To determine the role for the Rad16 RING domain in UV repair, mutations in several of these critical RING domain residues were constructed and tested for activity in vivo. As shown in Table 3, mutation of presumed zinc-coordinating cysteine residue 537, 540, 560, or 580 caused some degree of UV defect in vivo. rad16-C557A conferred wild-type UV survival but was still defective for interaction with Rad7 (Table 3). It is possible that Rad16 has a Rad7-independent function, but as the biochemical and genetic data strongly favor an exclusive function for Rad16 in a complex with Rad7 (20, 52), these results suggest instead that the rad16-C557A-Rad7 complex is intact but weakened in vivo and is destabilized during the coimmunoprecipitation procedure.

All of the other mutations destabilized the interaction between Rad16 and Rad7, as judged by immunoprecipitation experiments (Table 3), but it was unclear if the RING domain participates directly in the interaction with Rad7 or if the defects resulted indirectly from instability of the Rad16 folded structure. To distinguish between these possibilities, RING domain residue Y564 was mutated to alanine. Y564 is analogous to a solvent-exposed hydrophobic residue, W408, in the c-Cbl RING domain (81) and Y944 in Rad5 (69), which are essential for interaction with the E2s UbcH7 and Ubc13, respectively. Unexpectedly, rad16-Y564A did not confer a UV-sensitive phenotype in otherwise wild-type cells (Fig. 3A). As modeling studies predicted that Y564 would be critical for an interaction between the RING domain and another protein, these results suggest that mutations of zinc-coordinating cysteine residues do destabilize the folded structure of Rad16, but the RING domain interaction surface per se is not required for NEF4 function in otherwise wild-type cells.

Functional overlap of the Rad16 RING domain and Rad23 in NER. One explanation for the wild-type UV sensitivity of the *rad16-Y564A* strain is that another activity can compensate for the RING defect. Previous genetic analyses revealed phenotypic similarities between *rad16*, *rad7*, and *rad23* strains (48, 76). Rad23 possesses ubiquitin-binding domains, has a ubiquitin-like N-terminal domain, and is associated with the proteasome (72). These observations suggested that Rad23 might compensate for defects in NEF4. As shown in Fig. 3B, in marked contrast to the wild-type activity of *rad16-Y564A* in *RAD23* cells, *rad16-Y564A* displayed a strong synthetic UV defect in *rad23*Δ cells. Deleting *RAD16* resulted in roughly the same degree of UV sensitivity in *RAD23* and *rad23*Δ cells; in some strain backgrounds, the loss of both *RAD16* and *RAD23* resulted in somewhat enhanced UV sensitivity compared to the single mutants alone (see Fig. 8, discussed below, and data not shown). The combined results of Fig. 3A and B are consistent with the hypothesis that Rad16 possesses more than one biochemical activity; only one of these activities requires Rad16-Y564 and is functionally redundant with Rad23.

All of the other Rad16 RING domain mutants also conferred synthetic UV sensitivity when tested in *rad23*Δ cells (Table 3). Rad7 and rad16-Y564A associate in vivo, with only an approximate twofold decrease in coassociation in *rad23*Δ cells (Fig. 3C). Similar results were obtained when the immunoprecipitation was performed with extract from *RAD23* cells (not shown). Therefore, the rad16-Y564A defect is not due to disruption of the Rad16-Rad7 interaction, but instead these observations support the idea that the RING domain participates in some other function. In contrast to the results with the RING mutants, the UV sensitivity of a *rad23*Δ *rad16-K216A*

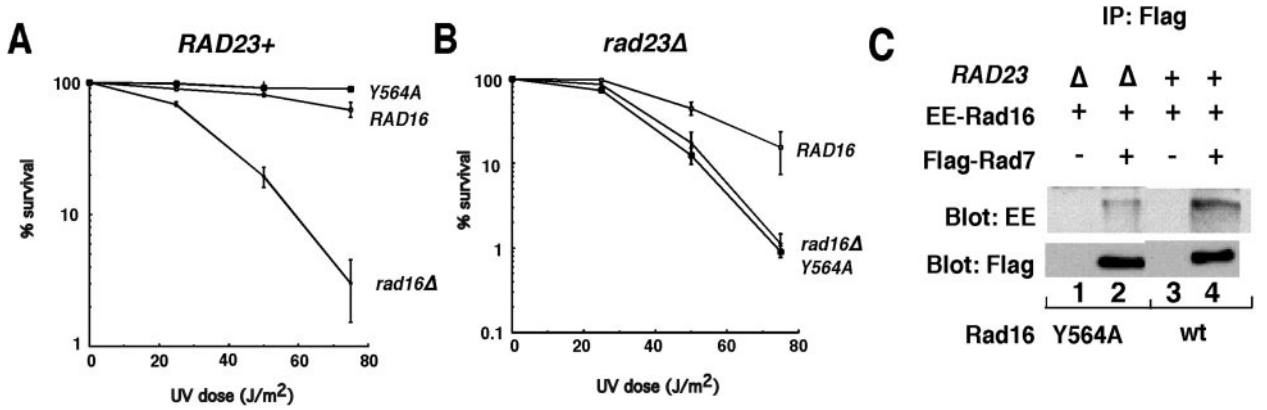

FIG. 3. Mutation of the RING domain impaired Rad16 function in vivo. (A) UV sensitivity of wild-type (*RAD16*), *rad16*Δ, and *rad16-Y564A* strains, determined as described for Fig. 2A. *rad16-Y564A* encodes a mutation in the RING domain. (B) UV sensitivity of *rad23*Δ strains with wild-type *RAD16*, *rad16*Δ, or *rad16-Y564A*. (C) Coimmunoprecipitation experiment performed as in Fig. 2D, but the reactions in lanes 1 and 2 were performed with extracts from *rad23*Δ cells harboring EE-tagged rad16-Y564. Note that Rad7 and rad16-Y564A coassociate in *rad23*Δ cells with only an approximate twofold decrease, as determined by densitometric analysis of the Western blot.

strain roughly reflected the additive UV sensitivities conferred by the individual mutations (Table 3). Additionally, the *rad16-K216A,Y564A* allele conferred moderate UV sensitivity in *RAD23* cells (reflecting loss of ATPase activity). This double point mutant had no detectable function in *rad23*Δ cells, reflecting the importance of the RING domain when Rad23 is absent (Table 3 and data not shown).

Function of the Rad7 F-box in NER. A similar analysis was performed to determine the role of the Rad7 F-box in NER. *rad7* alleles were constructed with point mutations in the F-box or with the entire F-box motif deleted (Table 3). As shown in Fig. 4A, a strain that contains *RAD7* with the whole F-box deleted (*rad7-*Δ*F-box*) was not sensitive to UV damage. Strikingly, however, a synthetic UV defect was observed in *rad23*Δ *rad7-*Δ*F-box* cells (Fig. 4B) that was quantitatively similar to the synthetic UV defect observed in *rad23*Δ *rad16-Y564A* cells (Fig. 3B). This result fits well with a previous report demonstrating a synthetic UV defect in *rad23*Δ cells carrying an allele of *rad7* with a large deletion of the 5′ end of the gene removing the newly identified F-box and additional sequences (48). As shown in Fig. 4C Rad16 was associated with rad7-ΔF-box in both *RAD23* and *rad23*Δ cells, indicating that the Rad7 F-box is not required for association with Rad16. Other alleles of *rad7* that encode point mutations in the Rad7 F-box motif were also tested (Table 3). rad7-W41A was not defective for UV repair, but rad7-I37A and the F-box double point mutant rad7-K40A,Q43A conferred synthetic UV defects in *rad23*Δ cells, and both proteins associated with Rad16, as judged by coimmunoprecipitation (Table 3 and Fig. 4D).

Genetic connection between ELC1 and NEF4. While this analysis was in progress, Elc1 was identified as a Rad7-associated protein (25). A human Elc1 homologue is a component of an E3 ubiquitin ligase that contains a RING domain subunit (37). Little is known about the function of Elc1 in *S. cerevisiae*, although it has been shown to regulate the degradation of stress proteins (31). These results suggest another link between NEF4 and a ubiquitin-mediated repair pathway. To determine if Elc1 functions with Rad16 and Rad7 in NER, various *elc1*Δ strains were tested for UV sensitivity. As shown in Fig. 5A, an *elc1*Δ strain was not sensitive to UV damage. However, an *elc1*Δ *rad23*Δ strain displayed the same synthetic UV sensitivity as was observed in *rad23*Δ strains with genes encoding rad16 RING or rad7 F-box mutations. As shown in Fig. 5B, a *rad7*Δ *elc1*Δ strain had the same UV sensitivity as a *rad7*Δ strain, and the triple deletion *rad7*Δ *rad23*Δ *elc1*Δ strain had the same UV sensitivity as the *rad7*Δ *rad23*Δ and *rad23*Δ *elc1*Δ strains. These results are consistent with the idea that Elc1 functions in the NEF4 pathway. To complete the analysis, the effect of *elc1*Δ on the UV sensitivity of various *rad16* strains was also examined (Fig. 5C). Loss of *ELC1* did not affect the UV sensitivity of a *rad16*Δ strain or a *rad16-K216A* strain. On the other hand, an *elc1*Δ *rad16-Y564A* strain had a weak but statistically significant UV defect compared to the *elc1*Δ and *rad16-Y564A* strains (compare Fig. 5C to 3A).

Elc1 is physically associated with Rad7 and Rad16. To determine the physical relationship between Elc1 and NEF4, the levels of Elc1, Rad7, and Rad16 proteins were analyzed in various mutant strains, and immunoprecipitation experiments were performed. As shown in Fig. 6A, deletion of *ELC1* resulted in greatly reduced levels of Rad7 protein. This result was surprising because an *elc1*Δ strain did not have enhanced UV sensitivity compared to wild-type cells (Fig. 5A). Since there are detectable, albeit low, levels of Rad7 in *elc1*Δ cells, and since loss of *ELC1* does not bypass the requirement for either *RAD7* or *RAD16* (Fig. 5 and data not shown), these results suggest that NEF4 function is retained in *elc1*Δ cells despite the low levels of Rad7 polypeptide.

One likely possibility is that *elc1*Δ cells possess a kinetic defect in the repair of UV damage, a suggestion that is consistent with the observation that *elc1*Δ cells were recently found to be UV sensitive with a competitive growth assay (22). Deletion of *RAD7* resulted similarly in nearly undetectable levels of Elc1 protein (Fig. 6B). In contrast, Rad16 protein levels were unaffected by loss of Elc1 or Rad7 (Fig. 6C). Northern analysis demonstrated that *RAD7* message levels were not affected by *elc1*Δ, and conversely, *ELC1* message levels were not affected by *rad7*Δ (not shown). These results suggested that Elc1 is a component of NEF4 and that loss of Elc1 or Rad7

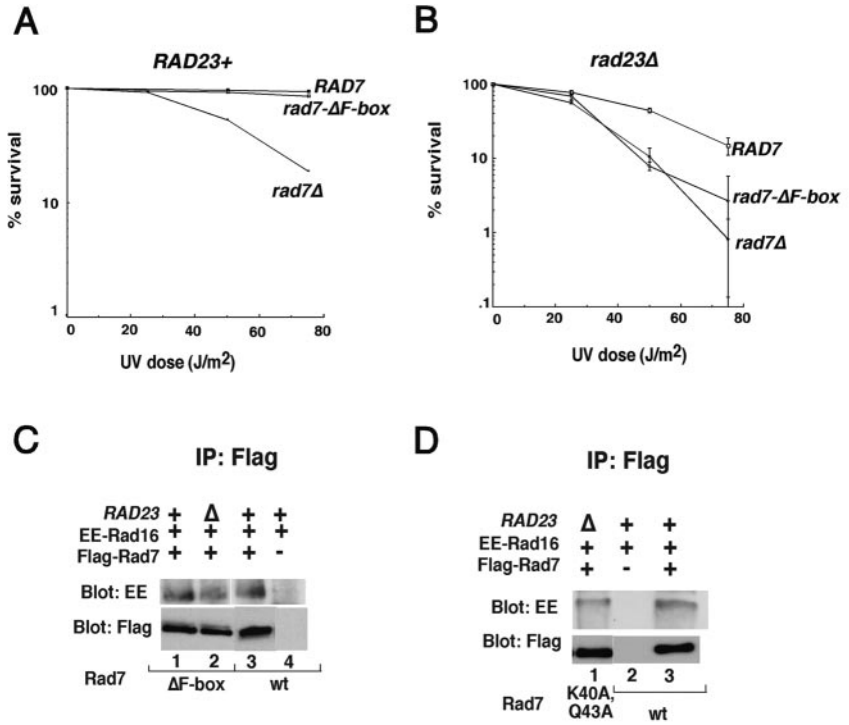

FIG. 4. Function of the Rad7 F-box. (A) UV sensitivity of wild-type (*RAD7*), *rad7-ΔF-box*, and *rad7*Δ strains. The experiment was performed as in Fig. 2A. (B) UV sensitivity of *rad23*Δ *RAD7*, *rad23*Δ *rad7-ΔF-box*, and *rad23*Δ *rad7*Δ strains, determined as described for Fig. 2A. Note that the *rad7-ΔF-box* allele is indistinguishable from *rad7*Δ in the *rad23*Δ background, whereas *rad7-ΔF-box* has wild-type activity in *RAD23* cells. (C) Rad7 F-box was not required for association of Rad7 with Rad16. Yeast whole-cell extracts with the indicated epitope-tagged proteins were used for immunoprecipitation with the Flag antibody, and Western blots of the immunoprecipitates were probed with the indicated antibodies. In lanes 1 to 3, the extracts contained Flag-tagged wild-type Rad7 or rad7-ΔF box. +, the protein was epitope tagged; −, untagged Rad7 (lane 4). All reaction mixtures contained EE-tagged Rad16, and extracts were made from cells with wild-type *RAD23* except lane 2, in which the extract was prepared from a *rad23*Δ strain. (D) rad7 F-box mutant K40A,Q43A associated with EE-tagged Rad16 in yeast whole-cell extracts. The experiment was performed as in C except lane 1 contains extracts from rad7-K40A,Q43A. *RAD23* was wild-type (+) or deleted from the strain (Δ), as indicated. In lane 2, wild-type Rad7 was untagged.

destabilized the NEF4 complex. As shown in Fig. 6D (lanes 1 and 2), Rad7 and Elc1 are physically associated in whole-cell extracts. This result is in good agreement with previous results (25). Furthermore, the Rad7-Elc1 interaction is independent of the Rad7 F-box (Fig. 6D, lanes 3 and 4). As shown in Fig. 6E and F, Rad7 and Rad16 were associated with immunoprecipitated Elc1, and Elc1 and Rad7 were associated with immunoprecipitated Rad16. Thus, Elc1, Rad7, and Rad16 are present in the same complex(es) in *S. cerevisiae* extracts.

Recombinant Elc1, Rad7, and/or Rad16 were coexpressed in

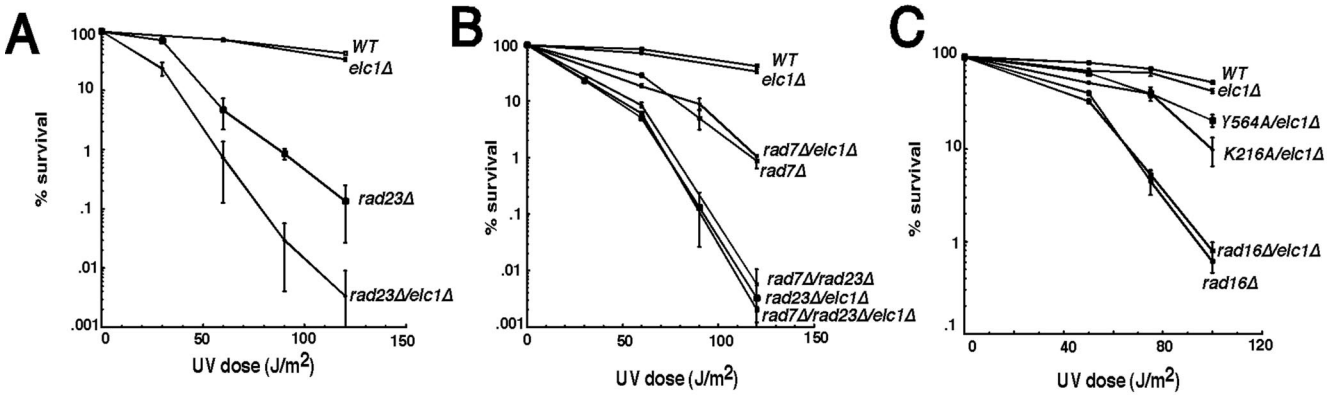

FIG. 5. Genetic interactions between *ELC1*, *RAD7*, *RAD16*, and *RAD23*. (A to C) The UV sensitivity of the indicated strains was determined by counting colonies derived from cells surviving irradiation at the indicated doses of UV light (see legend to Fig. 2A). Note that deletion of *ELC1* alone did not affect UV sensitivity, nor did it alter the UV sensitivity of *rad16*Δ, *rad7*Δ, or *rad7*Δ *rad23*Δ strains, whereas the *elc1*Δ *rad23*Δ strain is markedly more UV sensitive than the *rad23*Δ strain.

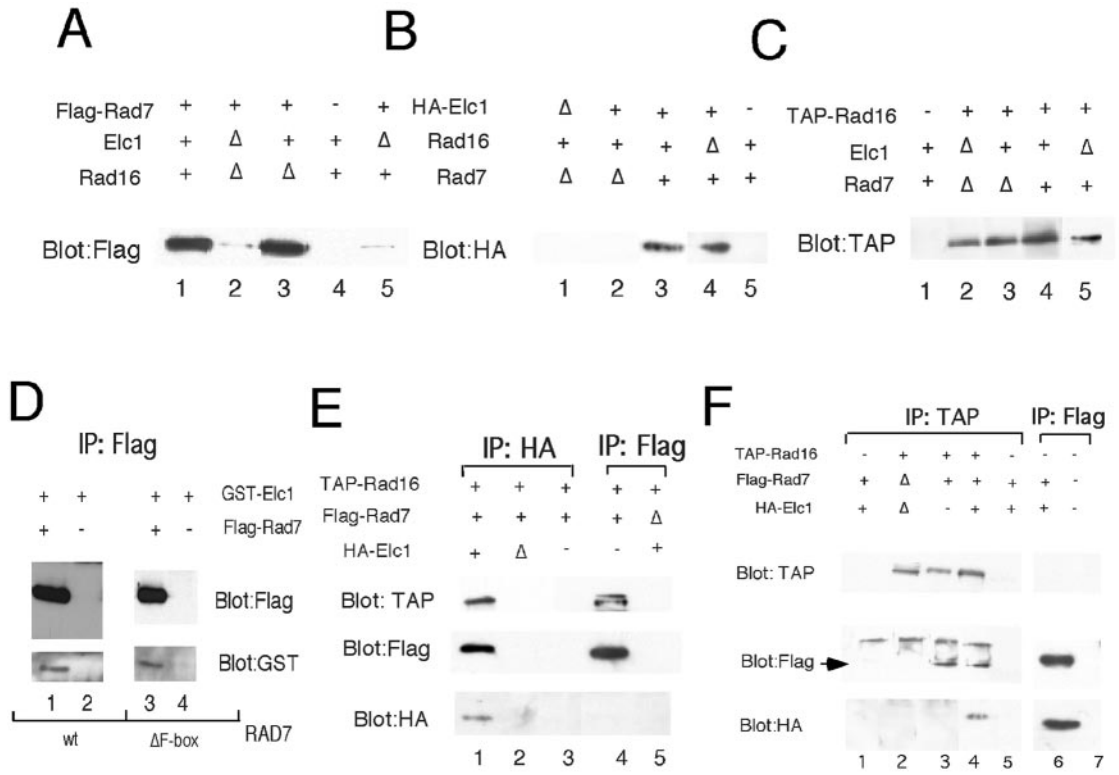

FIG. 6. Elc1 associated with Rad16 and Rad7 in yeast whole-cell extracts. (A) Immunoprecipitation of Flag-Rad7 from extracts with (lanes 1, 3, and 4) or without (lanes 2 and 5) Elc1 and with (lanes 1, 4, and 5) or without (lanes 2 and 3) Rad16. −, protein was present but untagged. Flag-Rad7 was detected by Western blotting with Flag antibody. (B) Similar to A except immunoprecipitation and Western blotting were performed with HA antibody with extract from an *elc1*Δ strain (lane 1), from an HA-Elc1 strain (lanes 2 to 4), or from a strain with untagged Elc1 (lane 5). Wild-type Rad7 and Rad16 were present (+) or absent (Δ) from the strains. (C) TAP-tagged Rad16 levels were determined in yeast whole-cell extracts by Western blotting with protein A antibodies. Extracts contained untagged Rad16 (lane 1) or TAP-tagged Rad16 (lanes 2 to 5). Wild-type *ELC1* and *RAD7* were present (+) or deleted (Δ) from the strains, as indicated. (D) Coimmunoprecipitation of GST-Elc1 and Flag-Rad7 from yeast whole-cell extracts with Flag antibodies. The experiment was performed as in Fig. 4C except that extracts contained GST-Elc1 with wild-type Rad7 (lanes 1 and 2) or Rad7-ΔF-box, Flag-tagged (+) or untagged (−), as indicated. Western blot analysis of Flag immunoprecipitates was performed with the indicated antibodies. (E and F) Reciprocal coimmunoprecipitation reactions demonstrate that Rad7, Rad16, and Elc1 are coassociated in yeast whole-cell extracts. (E) HA antibody was used for immunoprecipitation of HA-Elc1 in lanes 1 to 3, and Flag antibody was used for immunoprecipitation of Flag-Rad7 in lanes 4 and 5. (F) Protein A antibody was used for immunoprecipitation of TAP-Rad16 in lanes 1 to 5, and Flag antibody was used for immunoprecipitation of Flag-Rad7 in lanes 6 and 7.

bacterial cells and analyzed by affinity purification. Full-length Rad7 was expressed as a GST fusion, and cell lysates were incubated with glutathione-agarose in the presence or absence of full-length histidine-tagged Elc1 and Py-tagged Rad16. GST-Rad7 alone was poorly expressed (Fig. 7A, lane 2), although some GST-Rad7 binding to glutathione-agarose beads could be detected (Fig. 7B, lane 15). Elc1 and Rad16 did not bind to the glutathione beads, either alone or together (Fig. 7B, lanes 1, 2 and 5 to 8). On the other hand, Elc1 bound to GST-Rad7 in the absence of Rad16, and Rad16 was bound to Rad7 in the absence of Elc1 (Fig. 7B, lanes 9 to 12). When all three proteins were expressed in the same cell, all three were bound to glutathione agarose (Fig. 7B, lanes 13 and 14). Since Rad16 and Elc1 can bind to Rad7 independently, it was not possible to determine if all three recombinant proteins can form a discrete complex in this system, but Rad16-Rad7 and Rad7-Elc1 binary complexes can clearly assemble in the absence of other *S. cerevisiae* proteins.

Genetic interactions between RAD16 and certain *UBC* genes. If NEF4 is an E3, then an E2 must also function in the NEF4 repair pathway. Biochemical approaches have not identified an E2 that physically associates with NEF4 (15, 25), so a genetic approach was undertaken to identify E2s that might interact weakly or transiently with NEF4. Since mutations in the F-box and RING domains of NEF4 confer synthetic UV defects in *rad23*Δ cells, double mutant strains were constructed with a deletion of *RAD23* and a mutation in one of 13 E2-encoding *UBC* genes. The UV sensitivity of the double mutant strains was scored by a serial dilution spot assay. The results are summarized in Fig. 8. *rad23*Δ strains with deletions of *UBC2*/*RAD6* or *UBC13* had increased UV sensitivity compared to strains with any single gene deletion. A *rad23*Δ *ubc9-1* strain displayed a slight slow-growth phenotype in the absence of UV damage and increased UV sensitivity compared to either the *rad23*Δ or *ubc9-1* strain. No other double mutant strains had increased UV sensitivity, as would be expected for loss of an E2 that participates in the NEF4 pathway.

Both *UBC2*/*RAD6* and *UBC13* play roles in postreplication repair, which explains why *rad16*Δ *ubc2*Δ and *rad16*Δ *ubc13*Δ strains are more UV sensitive than strains missing any of the

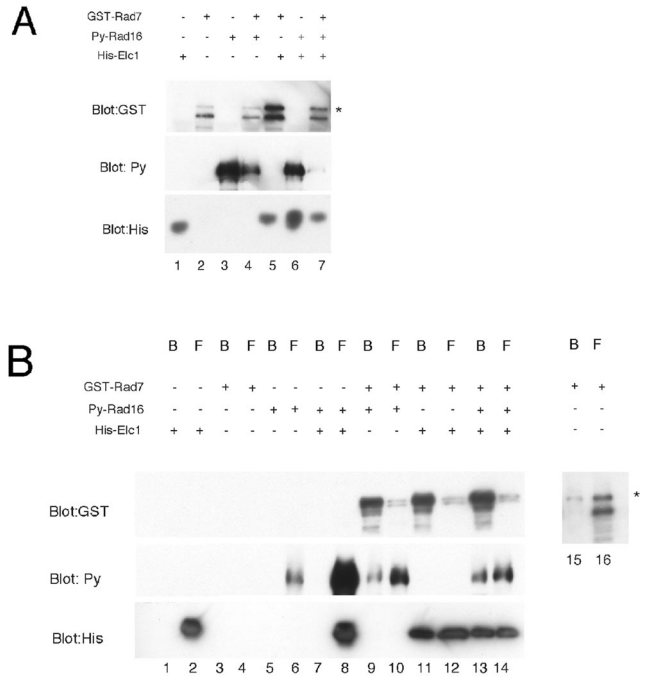

FIG. 7. Association of recombinant Rad16 and Elc1 with Rad7 in vitro. (A) Bacterial lysates were analyzed by Western blotting to detect the expression of recombinant GST-tagged Rad7, EE-tagged Rad16, and/or His-tagged Elc1. The proteins were expressed either alone or in combination, as indicated by the + and − symbols. Full-length GST-Rad7 is indicated by an asterisk. Note that significantly more GST-Rad7 was made when Elc1 or Elc1 and Rad16 were coexpressed with GST-Rad7 than when GST-Rad7 was expressed alone (lanes 5 and 7 compared to lane 2). (B) Western blot analysis of material bound to glutathione-agarose beads (B) and flowthrough (F) with the bacterial lysates in panel A. Lanes 15 and 16 are from a longer exposure of lanes 3 and 4. Note that GST-Rad7 alone was expressed poorly and did not bind well to glutathione-agarose beads. Similarly, His-Elc1 and EE-Rad16 did not bind to glutathione beads, either alone or in combination (lanes 1, 2, and 5 to 8). In contrast, GST-Rad7, His-Elc1, and EE-Rad16 were all bound to beads when GST-Rad7 was coexpressed with any combination of the other two (lanes 9 to 14).

single genes alone (Fig. 8). The enhanced UV defects in these double mutant strains could therefore be due solely to the combined defects in two repair pathways or could in principle be due to an additional, novel interaction with NEF4. To distinguish among these possibilities, the UV sensitivities of *rad16*Δ *rad23*Δ *ubc2*Δ, *rad16*Δ *rad23*Δ *ubc9-1*, and *rad16*Δ *rad23*Δ *ubc13*Δ triple mutant strains were compared to the UV sensitivities of the respective *rad23*Δ *ubc* strains (Fig. 8). The prediction was that loss of the NEF4 component Rad16 would not increase the UV sensitivity of a strain missing Rad23 and the E2 with which NEF4 interacts.

As shown in Fig. 8, the *rad16*Δ *rad23*Δ *ubc2*Δ strain had a severe growth defect in the absence of UV irradiation, and the comparative UV sensitivity of this strain could not be determined. In contrast, the UV sensitivity of the *rad16*Δ *rad23*Δ*ubc9-1* strain was very similar to that of the *rad23*Δ *ubc9-1* strain, and the sensitivity of the *rad16*Δ *rad23*Δ *ubc13*Δ strain was similar to that of the *rad23*Δ *ubc13*Δ strain. A similar epistatic relationship between *RAD16* and *UBC13* was also observed when double and triple mutant strains were tested with the *rad16-Y564A* allele rather than *rad16*Δ (data not shown). Thus, both *UBC9* and *UBC13* fulfill genetic criteria for participation in the NEF4 pathway. As an additional control for the specificity of these genetic interactions, no change in UV sensitivity was observed in *rad23*Δ and *rad16*Δ *rad23*Δ strains when *UBC8* was deleted (Fig. 8).

NEF4 regulates Rad4 levels and affects ubiquitylation of Rad23. Rad4 interacts with Rad7 by two-hybrid analysis (76), and the Rad4-Rad23 complex recognizes UV-damaged DNA (6, 68). These observations suggested that Rad4 could be a substrate for the inferred E3 activity of NEF4. To determine if NEF4 affects Rad4 levels during repair, cells were UV irradiated and harvested at various times thereafter. In wild-type cells, UV irradiation led to a five- to ninefold increase in Rad4 protein, as reported previously (Fig. 9A) (66). In *rad7*Δ cells, Rad4 levels were elevated in undamaged cells and remained high throughout the 2-h time course postirradiation (Fig. 9A). In contrast, Rad4 levels were induced about fourfold following irradiation of *rad23*Δ cells, but the induction of Rad4 levels was only transient. The levels of Rad4 in *rad7*Δ *rad23*Δ cells following irradiation were even more markedly reduced than in *rad23*Δ cells (Fig. 9A). The effect of *rad23*Δ on Rad4 levels fits well with recently published data (46), and the very low levels of Rad4 in UV-irradiated *rad7*Δ *rad23*Δ cells suggest an explanation for the synthetic UV sensitivity of this double mutant strain.

The most striking effect of *rad7*Δ in the above experiment was to cause Rad4 levels to be elevated in undamaged cells. As shown in Fig. 9B and C, Rad4 protein levels were also elevated in *elc1*Δ and *rad7-*Δ*F-box* cells. Rad4 levels were also assessed in undamaged *ubc13*Δ cells and *ubc9-1* cells at the permissive (23°C) and semipermissive (30°C) temperatures. The levels of Rad4 were elevated in *ubc13*Δ cells to a level that was comparable to the levels seen in the NEF4 mutant strains (Fig. 9B and C). This is consistent with the idea that Ubc13 interacts with NEF4. Surprisingly, Rad4 levels were very low in *ubc9-1* cells at the semipermissive temperature of 30°C (Fig. 9B and C), suggesting that while Ubc9 is involved in the regulation of Rad4 protein levels, it functions in a different pathway. The effect of *ubc9-1* on Rad4 protein levels is likely responsible, at least in part, for the UV sensitivity of the *ubc9-1* strain and the synthetic UV sensitivity of the *ubc9-1rad23*Δ strain.

To further test the relationship between NEF4 function and Rad4, the effects of *RAD16* mutations on Rad4 levels were determined. As shown in Fig. 9D, Rad4 levels are elevated in the *rad16*Δ strain compared to the wild-type strain. Rad4 levels were unaffected by the loss-of-function mutation in the Rad16 ATPase, K216A, indicating that ATPase activity is not required for turnover of Rad4. Rad4 levels were elevated, however, in the *rad16-Y564A* and *rad16-K216A,Y564A* strains, results that are fully consistent with the inferred function of the NEF4 E3 activity in Rad4 turnover. Finally, a role for NEF4 in control of *RAD4* transcription was tested directly. Deletion of *RAD7* did not affect *RAD4* message levels (not shown), consistent with the conclusion that NEF4 regulates Rad4 protein levels by a posttranscriptional mechanism.

Rad4 and Rad23 have been shown to be ubiquitylated and degraded by the 26S proteasome (39, 42, 59). To determine if the proteasome is required for NEF4-mediated turnover of Rad4, strains were constructed with a conditional mutation in

	BY4742 (wt)	rad16Δ	rad23Δ	rad16Δ/ rad23Δ
BY4742 (wt)	++++++	++++	++++	++±
rad16Δ	++++		++±	
rad23Δ	++++	++±		
ubc1Δ	++++++	++++	++++	n.d.
ubc2Δ (rad6Δ)	++++	+±	+±	–[a]
ubc3[ts] (cdc34)	+++++	+++±[a]	++++	n.d.
ubc4Δ	++++++	++++	++++	n.d.
ubc5Δ	++++++	++++	++++	n.d.
ubc6Δ	++++++	n.d.	++++	n.d.
ubc7Δ (qri8Δ)	++++++	n.d.	++++	n.d.
ubc8Δ	++++++	++++	++++	++
ubc9-1[ts]	++++	++±[a]	+±[a]	+±[a]
ubc10Δ (pex4Δ)	++++++	n.d.	++++	n.d.
ubc11Δ	++++++	n.d.	++++	n.d.
ubc12Δ	++++++	n.d.	++++	n.d.
ubc13Δ	+++++	+±	+±	+

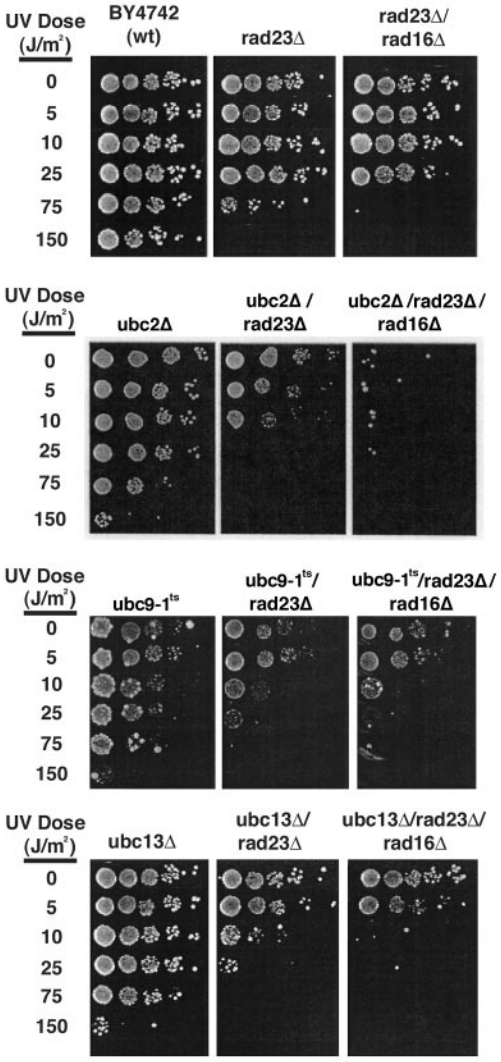

FIG. 8. Systematic analysis of UV sensitivities of *ubc* strains. UV sensitivity spot assays of various *ubc*, *ubc rad16*Δ, *ubc rad23*Δ, and *ubc rad16*Δ *rad23*Δ strains were performed, and the data are summarized on the left. Strains were ranked by degree of UV resistance as follows: ++++++, +++++, ++++, +++, ++, and + indicate growth at 150, 100, 75, 50, 10, and 5 J/m^2, respectively. Growth intermediate between two exposures is indicated by ±. Temperature-sensitive (ts) strains were tested at the semipermissive temperature (*ubc3* at 35°C and *ubc9-1* at 32°C). a, strains with growth defects in the absence of UV irradiation; n.d., not determined. Representative composite panels of the UV spot assays for a *rad23*Δ strain and *rad16*Δ *rad23*Δ strain along with *ubc2*Δ, *ubc9-1^{ts}*, or *ubc13*Δ are shown on the right.

CIM5 (*RPT1*), a gene encoding a component of the proteasome 19S regulatory cap (10). The 19S subunits Cim3 (Rpt6) and Cim5 were previously shown to cofractionate with Rad23 in *S. cerevisiae* (59), and mutation of *CIM5* stabilizes Rad23 (59). As expected, in undamaged cells, Rad4 levels were low in wild-type cells and elevated in *rad7*Δ cells (Fig. 9E). Rad4 levels were also elevated in *cim5* cells, consistent with the idea that Rad4 is degraded in a proteasome-dependent manner (Fig. 9E). Rad4 levels were equivalently elevated in *cim5*, *rad7*Δ, and *rad7*Δ *cim5* cells (Fig. 9E). This epistatic relationship provides support for a pathway in which NEF4 regulates turnover of Rad4 by directing it to the proteasome.

To determine if NEF4 also affects ubiquitylation or steady-state levels of Rad23, we first examined Rad23 by Western blotting extracts from wild-type cells following UV exposure. As shown in Fig. 10A, steady-state levels of Rad23 were not detectably affected by UV irradiation, but instead, UV irradiation led to the accumulation of slower-migrating, modified forms of Rad23 (compare lane 2 to lanes 3 to 6 or lane 8 to lanes 9 to 12). These modified forms of Rad23 are indistinguishable from the ubiquitylated forms of Rad23 previously reported by Madura and colleagues (39). As shown in Fig. 10B, the levels of Rad23 and its ubiquitylated forms were elevated in nonirradiated *rad7*Δ, *rad16*Δ, and *ubc13*Δ strains compared to wild-type and *ubc2*Δ cells. Thus, NEF4 function appears to antagonize ubiquitylation of Rad23.

DISCUSSION

Phenotypic redundancy and unique roles for NEF4 and Rad23 in NER. Previous analyses defined physical and genetic relationships between Rad7, Rad16, and Rad23 (55, 76). First,

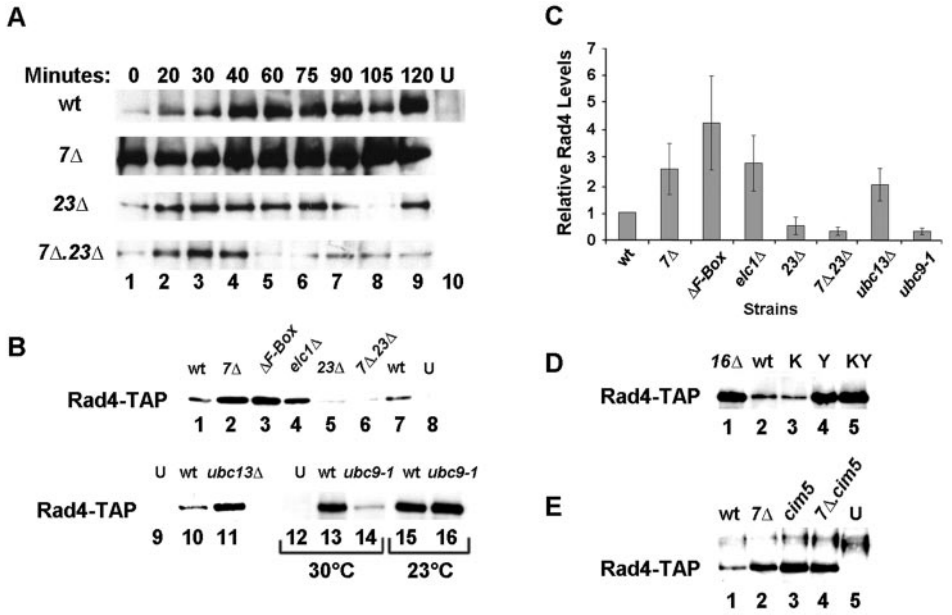

FIG. 9. Effect of NEF4 on Rad4 protein levels. (A) Western blot of Rad4-TAP in whole-cell extracts from wild-type (wt), *rad7*Δ (7Δ), *rad23*Δ *(*23Δ), and *rad7*Δ.*rad23*Δ (7Δ23Δ) strains harboring a chromosomal copy of Rad4 with a TAP epitope tag or wild-type cells in which Rad4 was untagged (U). Extracts were made from nonirradiated cells (lanes 1, zero minutes) or from cells irradiated with 100-J/m^2 UV light. Cells were harvested at the indicated times following UV irradiation. For all Western blots in this figure, equivalent loading of total protein was verified by staining the blots with Ponceau S (not shown). (B) Western blot of Rad4-TAP in whole-cell extracts from undamaged wild-type (wt), 7Δ, *rad7*Δ*F-Box* (Δ*F-Box*), *elc1*Δ, *rad23*Δ, *rad7*Δ*0.23*Δ, *ubc13*Δ, and *ubc9-1* strains. Extracts from cells harboring untagged Rad4 (U) are shown in lanes 8, 9, and 12. Extracts in lanes 1 to 11 were from cells grown at 30°C; extracts in lanes 12 to 16 were from cells grown at the temperatures indicated. Note that lanes 12 to 16 were from an exposure 30 times longer than that of lanes 1 to 11 to detect the low levels of Rad4-TAP in *ubc9-1* cells grown at 30°C (lane 14). (C) Quantitation of Rad4 levels in extracts from the indicated undamaged cells was performed by densitometric analysis of Western blots like the one in Fig. 9B. Rad4 levels were normalized to the wild-type level and corrected for background in the untagged strain. Data from the *ubc9-1* strain was obtained from cells grown at 30°C. The data were obtained from three to six separate experiments; error bars represent the standard deviation. (D) Western blot of Rad4-TAP in whole-cell extracts from undamaged wild-type (wt), *rad16*Δ (16Δ), *rad16-K216A* (K), *rad16-Y564A* (Y), or *rad16-K216A,Y564A* (KY) cells. (E) Western blot of Rad4-TAP in whole-cell extracts from undamaged wild-type (wt), *rad7*Δ (*7*Δ), *cim5*^{ts} (cim5), and *rad7*Δ *cim5*^{ts} (7Δ.cim5) cells or cells with untagged Rad4 (U). Cells were grown at the semipermissive temperature of 23°C prior to extract preparation.

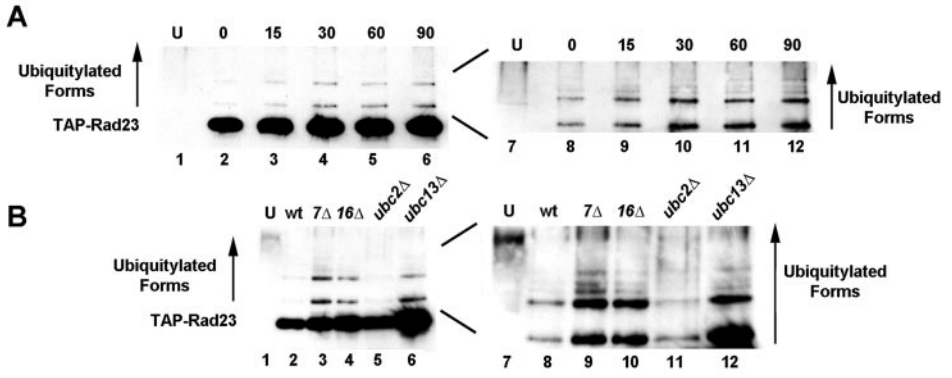

FIG. 10. Effects of NEF4 on modification of Rad23. (A) TAP-Rad23 Western blot of extracts from TAP-Rad23 wild-type cells (lanes 2 to 6 and 8 to 12) or wild-type cells in which Rad4 was untagged (U, lanes 1 and 7). Extracts in lanes 2 to 6 and 8 to 12 were prepared from unirradiated cells (lanes 2 and 8, zero minutes) or cells irradiated with 100-J/m^2 UV light that were harvested at the indicated times (minutes) following UV irradiation. Lanes 7 to 12 are the same as 1 to 6 except the blot was exposed six times longer to better visualize higher-molecular-weight species of TAP-Rad23. The assignment of slower-migrating Rad23 species as ubiquitylated forms follows from the published work of Madura and colleagues (39). For all Western blots in this figure, equivalent loading of total protein was verified by staining the blots with Ponceau S (not shown). (B) Western blot of TAP-Rad23 in whole-cell extracts from undamaged wild-type (wt, lanes 2 and 8), *rad7*Δ (7Δ, lanes 3 and 9), *rad16*Δ (16Δ, lanes 4 and 10), *ubc2*Δ (lanes 5 and 11), and *ubc13*Δ (lanes 6 and 12) strains harboring a chromosomal copy of Rad23 with a TAP epitope tag. Extract from wild-type cells in which Rad4 was untagged (U) is in lane 1. Lanes 7 to 12 are the same as 1 to 6 except the blot was exposed six times longer to better visualize the higher-molecular-weight species of TAP-Rad23.

there are phenotypic similarities between *rad7*, *rad16*, and *rad23* strains. For example, all three mutations confer a moderate degree of UV sensitivity and are involved in the repair of nontranscribed DNA (48, 51, 76). The results presented here provide a biochemical framework for understanding how these factors cooperate in NER. We propose that a central function of NEF4 is to regulate the levels of Rad4 and that Rad4 levels are coordinately regulated by the activities of NEF4 and Rad23. In addition, NEF4 has a unique role in NER that requires the Snf2/Swi2 ATPase activity of Rad16.

Rad23 has well-established roles in ubiquitin-mediated protein turnover (9) and was previously reported to regulate Rad4 protein levels (42, 46). Interestingly, the binding of Rad23 to ubiquitylated proteins inhibits ubiquitin chain elongation, resulting in protein stabilization (9, 24, 53, 66). This mechanism can explain in principle how Rad23 stabilizes Rad4 (42). In agreement with previous studies (42, 46), we observed that Rad4 levels are reduced in undamaged *rad23*Δ cells compared to a congenic wild-type strain. In undamaged cells, loss of NEF4 function allows Rad4 protein levels to accumulate. In addition, mutation of Cim5, a proteasomal subunit implicated in regulating stabilization of Rad23, causes Rad4 levels to be elevated similarly to that seen when NEF4 is crippled. Loss of NEF4 function has little effect on Rad4 levels in damaged cells; perhaps NEF4-mediated degradation of Rad4 is inhibited when cells are damaged. On the other hand, deletion of *RAD23* results in reduced accumulation of Rad4 following DNA damage, indicating that Rad23 inhibits Rad4 degradation regardless of whether the cells have sustained DNA damage.

In undamaged *rad7*Δ *rad23*Δ cells, the levels of Rad4 are reduced. When these cells are treated with UV light, Rad4 protein levels are weakly and transiently induced. The low levels of Rad4 protein in this double mutant offer a possible explanation for why these cells are so UV sensitive. The synthetic UV sensitivity of *rad23*Δ cells with defects in the RING domain, F-box domain, or Elc1 can also be explained by low Rad4 protein levels resulting from combined defects in these two Rad4 regulatory pathways. But if NEF4 is responsible for targeting Rad4 for ubiquitylation, why are Rad4 levels low in these double mutant strains? It is possible that the loss of two Rad4-interacting proteins, Rad7 and Rad23, causes instability of the Rad4 folded structure and leads to its degradation. Alternatively, there may be another pathway for specifically targeting Rad4 for degradation that has not been elucidated so far.

Interestingly, while the levels of the human Rad4 homologue, XPC, are also dictated by ubiquitin-mediated turnover controlled by Rad23 (46), there is no known NEF4 complex in human cells. The overall conservation of the NER machinery suggests that NEF4 probably does exist in humans, but its identification may be complicated by the large number of Snf2/Swi2-related and F-box family members. Biochemical analysis of human Elc1 may lead to the identification of a human NEF4 complex. Why are Rad4 protein levels normally maintained at a low level in undamaged cells? One possibility is that elevated levels of Rad4 in an undamaged cell might lead to inappropriate "repair" of normal replication and recombination intermediates (66). An alternative possibility is that low Rad4 levels allow Rad23 to be liberated for non-repair-related functions, although compared to Rad4, there is a vast excess of Rad23 in yeast cells (30).

New function for NEF4. It was reported that NEF4 has DNA-stimulated ATPase activity and displays ATP-dependent binding to damaged DNA (20, 21). These observations led to the hypothesis that NEF4 uses ATP hydrolysis to translocate along DNA as a scanning mechanism to locate DNA damage (20). As most nontranscribed DNA in *S. cerevisiae* is nucleosomal (41), this activity might also be used to remodel chromatin to allow access by the NER machinery. Here we report that Rad16 ATPase activity is indeed important for Rad16 function in vivo but that NEF4 regulates turnover of Rad4 as well. In this model, the ATPase activity of Rad16 provides a unique function in NER, whereas the E3 activity cooperates with Rad23 to regulate Rad4. As shown in Fig. 9A, loss of both Rad7 and Rad23 results in very low levels of Rad4 protein following UV damage. We propose that this explains the synthetic UV defect in these double mutant strains. In the absence of sufficient Rad4, the ATPase activity of Rad16 would be irrelevant because there is too little of the essential NER factor Rad4 to nucleate the assembly of repair complexes. This model can also explain why the *rad16-Y564A rad23*Δ cells have the same UV sensitivity as *rad16*Δ *rad23*Δ cells (Fig. 3A and B). Additionally, if the only unique function for Rad16 were its ATPase activity, then the *rad16*Δ and *rad16-K216A* alleles would cause the same UV sensitivity in *RAD23* cells. The fact that the *RAD16* deletion strain is more UV sensitive than the ATPase mutant suggests that NEF4 has another unique function which has yet to be discovered.

We propose that NEF4 controls Rad4 turnover by functioning as an E3 ubiquitin (or ubiquitin-like protein) ligase. While we have not yet been able to demonstrate E3 activity for NEF4 in vitro, six lines of evidence support the suggestion that NEF4 is an E3. First, two NEF4 subunits possess domains that are hallmarks for SCF-like ubiquitin ligases. The Rad16 RING domain is homologous to the RING domain of Rag1 (Fig. 1), a protein with demonstrated E3 activity in vitro (77). Rad7 has sequence similarity to other F-box proteins in both the F-box domain and in the C-terminal leucine-rich repeats (Fig. 1), strongly suggesting that Rad7 adopts an overall fold that is similar to the SCF subunit Grr1. Second, we report that Elc1 is a component of NEF4. Elc1 is related to the SCF component Skp1 (7), and elongin C is a component of certain mammalian E3s (8). Third, mutations in the RING and F-box domains and deletion of *ELC1* cause defects in the function of NEF4 consistent with loss of E3 activity, based on biochemical and structural studies of other E3s. Mutations in these motifs also display synthetic UV sensitivity when combined with a deletion of *RAD23*, a gene encoding a protein with a well-documented role in regulating ubiquitin-mediated protein turnover. Fourth, we provide genetic evidence for the involvement of two E2s in the NEF4 pathway, as expected if NEF4 functions as an E3. Fifth, mutations in NEF4 affect Rad4 protein levels, suggesting that Rad4 is a downstream target of NEF4 E3 activity. Finally, a mutation in a subunit of the 19S cap of the proteasome results in accumulation of Rad4 in undamaged cells to the same extent as observed in a *rad7*Δ strain, linking NEF4 control of Rad4 protein levels to the proteasome.

The combination of ATPase and ubiquitylation functions in NEF4 is reminiscent of the activity of the postreplication re-

pair factor Rad5 (27, 69). Like Rad16, Rad5 also contains ATPase and RING domains (36). Rad5 interacts with the RING domain-containing protein Rad18 and recruits the Mms2-Ubc13 heterodimer to chromatin (27, 70). One function of the Rad5-containing E3 is to direct modification of PCNA (27). As shown in Fig. 1, sequence analysis demonstrates that there are several other Snf2/Swi2-related ATPases in this subclass that contain RING domains. These factors play diverse but poorly understood roles in maintenance of silent DNA (79) and transcription (78). Thus, the combination of Snf2/Swi2 ATPase activity and E3 activity in the same functional complex appears to be a general strategy for controlling nucleic acid metabolism through coordinated action of ATP-driven "remodeling" and ubiquitylation.

NEF4 complex redefined. While this work was in progress, a physical interaction between Rad7 and Elc1 was reported (25). Whether Rad7 formed complexes with Elc1 and Rad16 independently was unknown, however. The immunoprecipitation experiments in Fig. 6 demonstrated that Elc1, Rad16, and Rad7 are coassociated in yeast extracts. We conclude that all three proteins are in the same complex or complexes. NEF4 purified from yeast extracts was previously reported to behave as a discrete species composed of Rad7 and Rad16 proteins in a 1:1 stoichiometry (21). The results in Fig. **7** indicate that Elc1 and Rad16 can interact with Rad7 independently, and it is likely that Elc1 was not detected previously in native NEF4 simply because of its very small size. The role for Elc1 in NER is consistent with a recent study that demonstrated a function for Elc1 in the *S. cerevisiae* UV response in a competitive growth assay (22). Amplification of elongin C has been reported in certain prostate and breast cancers (50); a functional role for elongin C in cancer may be related to its function in NER, as genomic instability arising from defects in DNA repair is a hallmark of many types of cancer (56).

Architecture of NEF4. The analysis of NEF4 complexes in various *rad7*, *rad16*, and *elc1* mutant strains suggests an unusual arrangement of subunits compared to other well-characterized E3s. In SCF complexes, the F-box interacts with several subunits, including the RING domain-containing subunit (80). In NEF4, however, deletion of the F-box does not impair the interaction between Rad7 and the RING domain-containing subunit Rad16. Elc1 is distantly related to Skp1 but is missing the C-terminal portion of Skp1 that is required for its interaction with the F-box (63). Consequently, it is not surprising that the Rad7 F-box is not required for interaction with Elc1. The Rad7 F-box is in the region of Rad7 that was shown to interact with Rad4 via a two-hybrid assay (76), and the accumulation of Rad4 levels in the *rad7-ΔF-box* strain suggests that the function of the Rad7 F-box is to interact with Rad4 rather than with Rad16 or Elc1. Elc1 possesses secondary structural elements H2, S3, and H5 that are present in Skp1 and provide the surface for interaction with Cul1 (80). However, the Skp1 residues that mediate its interaction with Cul1 are not well conserved in Elc1 (not shown).

Could there be a cullin that assembles with NEF4? The native molecular weight of NEF4 is not consistent with the presence of a cullin (21), and a cullin was not associated with either native Rad7 (25) or Rad16 (15) complexes purified from *S. cerevisiae*. We performed genetic analyses to determine if one of the three yeast cullins might participate in the NEF4 repair pathway. The results from these studies do not support a role for a cullin in NEF4 function (see supplemental Fig. 1 and 2 at http://www.people.virginia.edu/~dta4n/auble_lab/Ramsey_et_al_supplement4.html). Together, these results indicate that neither a cullin nor Skp1 is a component of NEF4, and furthermore, the Rad7 F-box likely interacts with Rad4.

New roles for Ubc9 and Ubc13 in NER. If NEF4 functions as an E3, then it must recruit an E2 for modification of one or more substrates. None of the E2s in *S. cerevisiae* have been implicated in NEF4 function by previous biochemical or genetic analyses. The failure to identify a stable interaction between an E2 and NEF4 by a biochemical approach is perhaps not surprising because the enzymatic cycle leading to multiubiquitylation involves a cycle of E2-E3 association and dissociation (11). Identification of an E2 that works in conjunction with NEF4 is complicated genetically by the involvement of several E2s in other repair pathways and the phenotypic redundancy of Rad23 and the NEF4 E3 activity. Nonetheless, our analysis identified two *UBC* genes, *UBC9* and *UBC13*, which fulfill the requirements for participation in the NEF4 pathway. Ubc9 is responsible for conjugation of Smt3, the yeast SUMO homologue (35). Rad4 levels are very low in *ubc9-1* cells, indicating that Ubc9 functions in a pathway to stabilize Rad4. As Rad23 also stabilizes Rad4, one possibility is that Smt3/SUMO modification of Rad4 or Rad23 is important for Rad4 stability. Interestingly, while a physical interaction between Ubc9 and Rad23 has not been reported, an interaction between these two proteins is predicted by meta-analysis of yeast biochemical, expression, and interaction data (33) (data not shown).

Ubc13, in contrast, has a well-defined role in postreplication repair and functions with its heterodimeric partner Mms2 to catalyze the addition of lysine 63-linked ubiquitin chains to substrates (29). In contrast to lysine 48-linked chains, covalent modification by Ubc13-Mms2 does not lead to degradation of the modified target protein (28). Thus, neither Ubc9 nor Ubc13 is known to be involved in targeting substrates for degradation directly; instead, they are thought to regulate other properties of their substrates. Ubc9 and Ubc13 both participate in postreplication repair by modifying the same residue on PCNA to facilitate its different functions in replication and repair (27). Similarly, NEF4 may regulate Rad4 levels indirectly by altering the activity of another factor through SUMO or lysine 63-linked multiubiquitylation. Ubiquitylation of Rad23 is enhanced in NEF4- and Ubc13-defective cells, indicating that NEF4 is not directly responsible for these modifications of Rad23. If NEF4 regulates Rad4 levels directly, then accumulation of Rad4 might trigger the ubiquitylation of Rad23. Alternatively, the levels of Rad4 might be determined by the modification status of Rad23, which could itself be dictated by the modification status of an unknown substrate for NEF4.

Some rules for predicting RING domain-Ubc interactions emerged from the structure of the c-Cbl RING-UbcH7 complex (81). In particular, a hydrophobic residue at the position of residue Y564 in Rad16 is critical for the interaction between c-Cbl and UbcH7 and between Rad5 and Ubc13, and the nature of the residue at that position allows RING domains to discriminate among different Ubcs (69, 80, 81). Importantly, the Rad5-Ubc13 interaction depends on a tyrosine residue at

this position (69), so the suggestion that the Rad16 RING domain physically interacts with Ubc13 is compatible with structural as well as genetic data. As *ubc13*Δ affects Rad4 and Rad23 proteins similarly to E3 mutations in NEF4, we favor the idea that Ubc13 interacts directly with NEF4. It is of course possible that NEF4 interacts with more than one E2; for instance, Ubc4 and Ubc5 are highly related and have overlapping functions (64).

The emerging evidence indicates that there are several roles for the proteasome in NER. In addition to the roles of Rad23 and NEF4 in Rad4 turnover, there is also support for a nonproteolytic role for the proteasome (57). Both proteolytic and chaperone-like functions for the proteasome could therefore contribute to disassembling complexes bound to damaged DNA during the repair reaction. Interestingly, the mammalian DDB2 and Cockayne syndrome group A complexes possess ubiquitin ligase activities that are regulated by the COP9 signalosome (18). As DDB2 and Cockayne syndrome group A play critical roles in NER, the links between damage recognition and ubiquitin appear to extend to other NER pathways.

ACKNOWLEDGMENTS

We are grateful to Brehon Laurent, Dan Gietz, Linda Hyman, Chris Koth, Mike Tyers, Mark Goebl, Mark Hochstrasser, Mary Ann Osley, Cecile Pickart, Alex Varshavsky, and Mitch Smith for the plasmids and yeast strains used in this study. We are also grateful to Justin Reese for advice on sequence analysis, Mitch Smith for critically reading the manuscript, Sarah Juedes for help with plasmid preparation and strain construction, Rick Wood and Cecile Pickart for advice and encouragement, and members of the Auble lab for helpful discussions.

This work was supported by grants from the NIH (GM55763), March of Dimes, and Kincaid Charitable Trust and an Institutional Research Award from the American Cancer Society to D.T.A.

REFERENCES

1. **Aboussekhra, A., M. Biggerstaff, M. K. Shivji, J. A. Vilpo, V. Moncollin, V. N. Podust, M. Protic, U. Hubscher, J. M. Egly, and R. D. Wood.** 1995. Mammalian DNA nucleotide excision repair reconstituted with purified protein components. Cell **80:**859–868.
2. **Araujo, S. J., and R. D. Wood.** 1999. Protein complexes in nucleotide excision repair. Mutat. Res. **435:**23–33.
3. **Aravind, L., L. M. Iyer, and E. V. Koonin.** 2003. Scores of RINGS but no PHDs in ubiquitin signaling. Cell Cycle **2:**123–126.
4. **Auble, D. T., D. Wang, K. W. Post, and S. Hahn.** 1997. Molecular analysis of the SNF2/SWI2 protein family member MOT1, an ATP-driven enzyme that dissociates TATA-binding protein from DNA. Mol. Cell. Biol. **17:**4842–4851.
5. **Bang, D. D., R. Verhage, N. Goosen, J. Brouwer, and P. van de Putte.** 1992. Molecular cloning of RAD16, a gene involved in differential repair in Saccharomyces cerevisiae. Nucleic Acids Res. **20:**3925–3931.
6. **Batty, D. P., and R. D. Wood.** 2000. Damage recognition in nucleotide excision repair of DNA. Gene **241:**193–204.
7. **Botuyan, M. V., C. M. Koth, G. Mer, A. Chakrabartty, J. W. Conaway, R. C. Conaway, A. M. Edwards, C. H. Arrowsmith, and W. J. Chazin.** 1999. Binding of elongin A or a von Hippel-Lindau peptide stabilizes the structure of yeast elongin C. Proc. Natl. Acad. Sci. USA **96:**9033–9038.
8. **Brower, C. S., S. Sato, C. Tomomori-Sato, T. Kamura, A. Pause, R. Stearman, R. D. Klausner, S. Malik, W. S. Lane, I. Sorokina, R. G. Roeder, J. W. Conaway, and R. C. Conaway.** 2002. Mammalian mediator subunit mMED8 is an Elongin BC-interacting protein that can assemble with Cul2 and Rbx1 to reconstitute a ubiquitin ligase. Proc. Natl. Acad. Sci. USA **99:**10353–10358.
9. **Chen, L., and K. Madura.** 2002. Rad23 promotes the targeting of proteolytic substrates to the proteasome. Mol. Cell. Biol. **22:**4902–4913.
10. **Coux, O., K. Tanaka, and A. L. Goldberg.** 1996. Structure and functions of the 20S and 26S proteasomes. Annu. Rev. Biochem. **65:**801–847.
11. **Deffenbaugh, A. E., K. M. Scaglione, L. Zhang, J. M. Moore, T. Buranda, L. A. Sklar, and D. Skowyra.** 2003. Release of ubiquitin-charged Cdc34-S-Ub from the RING domain is essential for ubiquitination of the SCF(Cdc4)-bound substrate Sic1. Cell **114:**611–622.
12. **de Laat, W. L., N. G. Jaspers, and J. H. Hoeijmakers.** 1999. Molecular mechanism of nucleotide excision repair. Genes Dev. **13:**768–785.
13. **Eisen, J. A., K. S. Sweder, and P. C. Hanawalt.** 1995. Evolution of the SNF2 family of proteins: subfamilies with distinct sequences and functions. Nucleic Acids Res. **23:**2715–2723.
14. **Friedberg, E. C., A. J. Bardwell, L. Bardwell, W. J. Feaver, R. D. Kornberg, J. Q. Svejstrup, A. E. Tomkinson, and Z. Wang.** 1995. Nucleotide excision repair in the yeast Saccharomyces cerevisiae: its relationship to specialized mitotic recombination and RNA polymerase II basal transcription. Phil. Trans. R. Soc. London B Biol. Sci. **347:**63–68.
15. **Gavin, A. C., M. Bosche, R. Krause, P. Grandi, M. Marzioch, A. Bauer, J. Schultz, J. M. Rick, A. M. Michon, C. M. Cruciat, M. Remor, C. Hofert, M. Schelder, M. Brajenovic, H. Ruffner, A. Merino, K. Klein, M. Hudak, D. Dickson, T. Rudi, V. Gnau, A. Bauch, S. Bastuck, B. Huhse, C. Leutwein, M. A. Heurtier, R. R. Copley, A. Edelmann, E. Querfurth, V. Rybin, G. Drewes, M. Raida, T. Bouwmeester, P. Bork, B. Seraphin, B. Kuster, G. Neubauer, and G. Superti-Furga.** 2002. Functional organization of the yeast proteome by systematic analysis of protein complexes. Nature **415:**141–147.
16. **Goldstein, A. L., and J. H. McCusker.** 1999. Three new dominant drug resistance cassettes for gene disruption in Saccharomyces cerevisiae. Yeast **15:**1541–1553.
17. **Green, C. M., and G. Almouzni.** 2002. When repair meets chromatin. First in series on chromatin dynamics. EMBO Rep. **3:**28–33.
18. **Groisman, R., J. Polanowska, I. Kuraoka, J. Sawada, M. Saijo, R. Drapkin, A. F. Kisselev, K. Tanaka, and Y. Nakatani.** 2003. The ubiquitin ligase activity in the DDB2 and CSA complexes is differentially regulated by the COP9 signalosome in response to DNA damage. Cell **113:**357–367.
19. **Guzder, S. N., Y. Habraken, P. Sung, L. Prakash, and S. Prakash.** 1995. Reconstitution of yeast nucleotide excision repair with purified Rad proteins, replication protein A, and transcription factor TFIIH. J. Biol. Chem. **270:**12973–12976.
20. **Guzder, S. N., P. Sung, L. Prakash, and S. Prakash.** 1998. The DNA-dependent ATPase activity of yeast nucleotide excision repair factor 4 and its role in DNA damage recognition. J. Biol. Chem. **273:**6292–6296.
21. **Guzder, S. N., P. Sung, L. Prakash, and S. Prakash.** 1997. Yeast Rad7-Rad16 complex, specific for the nucleotide excision repair of the nontranscribed DNA strand, is an ATP-dependent DNA damage sensor. J. Biol. Chem. **272:**21665–21668.
22. **Hanway, D., J. K. Chin, G. Xia, G. Oshiro, E. A. Winzeler, and F. E. Romesberg.** 2002. Previously uncharacterized genes in the UV- and MMS-induced DNA damage response in yeast. Proc. Natl. Acad. Sci. USA **99:**10605–10610.
23. **He, Z., J. M. Wong, H. S. Maniar, S. J. Brill, and C. J. Ingles.** 1996. Assessing the requirements for nucleotide excision repair proteins of Saccharomyces cerevisiae in an in vitro system. J. Biol. Chem. **271:**28243–28249.
24. **Hiyama, H., M. Yokoi, C. Masutani, K. Sugasawa, T. Maekawa, K. Tanaka, J. H. Hoeijmakers, and F. Hanaoka.** 1999. Interaction of hHR23 with S5a. The ubiquitin-like domain of hHR23 mediates interaction with S5a subunit of 26 S proteasome. J. Biol. Chem. **274:**28019–28025.
25. **Ho, Y., A. Gruhler, A. Heilbut, G. D. Bader, L. Moore, S. L. Adams, A. Millar, P. Taylor, K. Bennett, K. Boutilier, L. Yang, C. Wolting, I. Donaldson, S. Schandorff, J. Shewnarane, M. Vo, J. Taggart, M. Goudreault, B. Muskat, C. Alfarano, D. Dewar, Z. Lin, K. Michalickova, A. R. Willems, H. Sassi, P. A. Nielsen, K. J. Rasmussen, J. R. Andersen, L. E. Johansen, L. H. Hansen, H. Jespersen, A. Podtelejnikov, E. Nielsen, J. Crawford, V. Poulsen, B. D. Sorensen, J. Matthiesen, R. C. Hendrickson, F. Gleeson, T. Pawson, M. F. Moran, D. Durocher, M. Mann, C. W. Hogue, D. Figeys, and M. Tyers.** 2002. Systematic identification of protein complexes in Saccharomyces cerevisiae by mass spectrometry. Nature **415:**180–183.
26. **Hochstrasser, M.** 1996. Ubiquitin-dependent protein degradation. Annu. Rev. Genet. **30:**405–439.
27. **Hoege, C., B. Pfander, G. L. Moldovan, G. Pyrowolakis, and S. Jentsch.** 2002. RAD6-dependent DNA repair is linked to modification of PCNA by ubiquitin and SUMO. Nature **419:**135–141.
28. **Hofmann, R. M., and C. M. Pickart.** 2001. In vitro assembly and recognition of Lys-63 polyubiquitin chains. J. Biol. Chem. **276:**27936–27943.
29. **Hofmann, R. M., and C. M. Pickart.** 1999. Noncanonical MMS2-encoded ubiquitin-conjugating enzyme functions in assembly of novel polyubiquitin chains for DNA repair. Cell **96:**645–653.
30. **Huh, W. K., J. V. Falvo, L. C. Gerke, A. S. Carroll, R. W. Howson, J. S. Weissman, and E. K. O'Shea.** 2003. Global analysis of protein localization in budding yeast. Nature **425:**686–691.
31. **Hyman, L. E., E. Kwon, S. Ghosh, J. McGee, A. M. Chachulska, T. Jackson, and W. H. Baricos.** 2002. Binding to Elongin C inhibits degradation of interacting proteins in yeast. J. Biol. Chem. **277:**15586–15591.
32. **Jackson, T., E. Kwon, A. M. Chachulska, and L. E. Hyman.** 2000. Novel roles for elongin C in yeast. Biochim. Biophys. Acta **1491:**161–176.
33. **Jansen, R., H. Yu, D. Greenbaum, Y. Kluger, N. J. Krogan, S. Chung, A. Emili, M. Snyder, J. F. Greenblatt, and M. Gerstein.** 2003. A Bayesian networks approach for predicting protein-protein interactions from genomic data. Science **302:**449–453.
34. **Joazeiro, C. A., and A. M. Weissman.** 2000. RING finger proteins: mediators of ubiquitin ligase activity. Cell **102:**549–552.

35. **Johnson, E. S., and G. Blobel.** 1997. Ubc9p is the conjugating enzyme for the ubiquitin-like protein Smt3p. J. Biol. Chem. **272:**26799–26802.
36. **Johnson, R. E., S. T. Henderson, T. D. Petes, S. Prakash, M. Bankmann, and L. Prakash.** 1992. *Saccharomyces cerevisiae RAD5*-encoded DNA repair protein contains DNA helicase and zinc-binding sequence motifs and affects the stability of simple repetitive sequences in the genome. Mol. Cell. Biol. **12:**3807–3818.
37. **Kamura, T., D. Burian, Q. Yan, S. L. Schmidt, W. S. Lane, E. Querido, P. E. Branton, A. Shilatifard, R. C. Conaway, and J. W. Conaway.** 2001. Muf1, a novel elongin BC-interacting leucine-rich repeat protein that can assemble with Cul5 and Rbx1 to reconstitute a ubiquitin ligase. J. Biol. Chem. **276:** 29748–29753.
38. **Koth, C. M., M. V. Botuyan, R. J. Moreland, D. B. Jansma, J. W. Conaway, R. C. Conaway, W. J. Chazin, J. D. Friesen, C. H. Arrowsmith, and A. M. Edwards.** 2000. Elongin from Saccharomyces cerevisiae. J. Biol. Chem. **275:** 11174–11180.
39. **Lambertson, D., L. Chen, and K. Madura.** 2003. Investigating the importance of proteasome-interaction for Rad23 function. Curr Genet. **42:**199–208.
40. **Li, S., and M. J. Smerdon.** 2004. Dissecting transcription coupled and global genomic repair in the chromatin of yeast GAL1–10 genes. J. Biol. Chem. **279:**14418–14426.
41. **Livingstone-Zatchej, M., R. Marcionelli, K. Moller, R. de Pril, and F. Thoma.** 2003. Repair of UV lesions in silenced chromatin provides in vivo evidence for a compact chromatin structure. J. Biol. Chem. **278:**37471–37479.
42. **Lommel, L., T. Ortolan, L. Chen, K. Madura, and K. S. Sweder.** 2002. Proteolysis of a nucleotide excision repair protein by the 26 S proteasome. Curr. Genet. **42:**9–20.
43. **Longtine, M. S., A. McKenzie, 3rd, D. J. Demarini, N. G. Shah, A. Wach, A. Brachat, P. Philippsen, and J. R. Pringle.** 1998. Additional modules for versatile and economical PCR-based gene deletion and modification in Saccharomyces cerevisiae. Yeast **14:**953–961.
44. **Lorick, K. L., J. P. Jensen, S. Fang, A. M. Ong, S. Hatakeyama, and A. M. Weissman.** 1999. RING fingers mediate ubiquitin-conjugating enzyme (E2)-dependent ubiquitination. Proc. Natl. Acad. Sci. USA **96:**11364–11369.
45. **Mueller, J. P., and M. J. Smerdon.** 1995. Repair of plasmid and genomic DNA in a rad7 delta mutant of yeast. Nucleic Acids Res. **23:**3457–3464.
46. **Ng, J. M., W. Vermeulen, G. T. van der Horst, S. Bergink, K. Sugasawa, H. Vrieling, and J. H. Hoeijmakers.** 2003. A novel regulation mechanism of DNA repair by damage-induced and RAD23-dependent stabilization of xeroderma pigmentosum group C protein. Genes Dev. **17:**1630–1645.
47. **Paetkau, D. W., J. A. Riese, W. S. MacMorran, R. A. Woods, and R. D. Gietz.** 1994. Interaction of the yeast RAD7 and SIR3 proteins: implications for DNA repair and chromatin structure. Genes Dev. **8:**2035–2045.
48. **Perozzi, G., and S. Prakash.** 1986. *RAD7* gene of *Saccharomyces cerevisiae*: transcripts, nucleotide sequence analysis, and functional relationship between the *RAD7* and *RAD23* gene products. Mol. Cell. Biol. **6:**1497–1507.
49. **Peterson, C. L.** 2000. ATP-dependent chromatin remodeling: going mobile. FEBS Lett. **476:**68–72.
50. **Porkka, K., O. Saramaki, M. Tanner, and T. Visakorpi.** 2002. Amplification and overexpression of elongin C gene discovered in prostate cancer by cDNA microarrays. Lab. Investig. **82:**629–637.
51. **Prakash, S., and L. Prakash.** 2000. Nucleotide excision repair in yeast. Mutat. Res. **451:**13–24.
52. **Prakash, S., P. Sung, and L. Prakash.** 1993. DNA repair genes and proteins of Saccharomyces cerevisiae. Annu. Rev. Genet. **27:**33–70.
53. **Raasi, S., and C. M. Pickart.** 2003. Rad23 ubiquitin-associated domains (UBA) inhibit 26 S proteasome-catalyzed proteolysis by sequestering lysine 48-linked polyubiquitin chains. J. Biol. Chem. **278:**8951–8959.
54. **Rigaut, G., A. Shevchenko, B. Rutz, M. Wilm, M. Mann, and B. Seraphin.** 1999. A generic protein purification method for protein complex characterization and proteome exploration. Nat. Biotechnol. **17:**1030–1032.
55. **Rodriguez, K., J. Talamantez, W. Huang, S. H. Reed, Z. Wang, L. Chen, W. J. Feaver, E. C. Friedberg, and A. E. Tomkinson.** 1998. Affinity purification and partial characterization of a yeast multiprotein complex for nucleotide excision repair using histidine-tagged Rad14 protein. J. Biol. Chem. **273:**34180–34189.
56. **Rouse, J., and S. P. Jackson.** 2002. Interfaces between the detection, signaling, and repair of DNA damage. Science **297:**547–551.
57. **Russell, S. J., S. H. Reed, W. Huang, E. C. Friedberg, and S. A. Johnston.** 1999. The 19S regulatory complex of the proteasome functions independently of proteolysis in nucleotide excision repair. Mol. Cell **3:**687–695.
58. **Saurin, A. J., K. L. Borden, M. N. Boddy, and P. S. Freemont.** 1996. Does this have a familiar RING? Trends Biochem. Sci. **21:**208–214.
59. **Schauber, C., L. Chen, P. Tongaonkar, I. Vega, D. Lambertson, W. Potts, and K. Madura.** 1998. Rad23 links DNA repair to the ubiquitin/proteasome pathway. Nature **391:**715–718.
60. **Schild, D., B. J. Glassner, R. K. Mortimer, M. Carlson, and B. C. Laurent.** 1992. Identification of RAD16, a yeast excision repair gene homologous to the recombinational repair gene RAD54 and to the SNF2 gene involved in transcriptional activation. Yeast **8:**385–395.
61. **Schneider, K. R., R. L. Smith, and E. K. O'Shea.** 1994. Phosphate-regulated inactivation of the kinase PHO80-PHO85 by the CDK inhibitor PHO81. Science **266:**122–126.
62. **Schneider, R., and M. Schweiger.** 1991. The yeast DNA repair proteins RAD1 and RAD7 share similar putative functional domains. FEBS Lett. **283:**203–206.
63. **Schulman, B. A., A. C. Carrano, P. D. Jeffrey, Z. Bowen, E. R. Kinnucan, M. S. Finnin, S. J. Elledge, J. W. Harper, M. Pagano, and N. P. Pavletich.** 2000. Insights into SCF ubiquitin ligases from the structure of the Skp1-Skp2 complex. Nature **408:**381–386.
64. **Seufert, W., and S. Jentsch.** 1991. Yeast ubiquitin-conjugating enzymes involved in selective protein degradation are essential for cell viability. Acta Biol. Hung. **42:**27–37.
65. **Sikorski, R. S., and P. Hieter.** 1989. A system of shuttle vectors and yeast host strains designed for efficient manipulation of DNA in Saccharomyces cerevisiae. Genetics **122:**19–27.
66. **Sweder, K., and K. Madura.** 2002. Regulation of repair by the 26S proteasome. J. Biomed. Biotechnol. **2:**94–105.
67. **Terleth, C., P. Schenk, R. Poot, J. Brouwer, and P. van de Putte.** 1990. Differential repair of UV damage in *rad* mutants of *Saccharomyces cerevisiae*: a possible function of G_2 arrest upon UV irradiation. Mol. Cell. Biol. **10:** 4678–4684.
68. **Thoma, F.** 1999. Light and dark in chromatin repair: repair of UV-induced DNA lesions by photolyase and nucleotide excision repair. EMBO J. **18:** 6585–6598.
69. **Ulrich, H. D.** 2003. Protein-protein interactions within an E2-RING finger complex. Implications for ubiquitin-dependent DNA damage repair. J. Biol. Chem. **278:**7051–7058.
70. **Ulrich, H. D., and S. Jentsch.** 2000. Two RING finger proteins mediate cooperation between ubiquitin-conjugating enzymes in DNA repair. EMBO J. **19:**3388–3397.
71. **Ura, K., and J. J. Hayes.** 2002. Nucleotide excision repair and chromatin remodeling. Eur. J. Biochem. **269:**2288–2293.
72. **van Laar, T., A. J. van der Eb, and C. Terleth.** 2002. A role for Rad23 proteins in 26S proteasome-dependent protein degradation? Mutat. Res. **499:**53–61.
73. **Verhage, R., A. M. Zeeman, N. de Groot, F. Gleig, D. D. Bang, P. van de Putte, and J. Brouwer.** 1994. The *RAD7* and *RAD16* genes, which are essential for pyrimidine dimer removal from the silent mating type loci, are also required for repair of the nontranscribed strand of an active gene in *Saccharomyces cerevisiae*. Mol. Cell. Biol. **14:**6135–6142.
74. **Vignali, M., A. H. Hassan, K. E. Neely, and J. L. Workman.** 2000. ATP-dependent chromatin-remodeling complexes. Mol. Cell. Biol. **20:**1899–1910.
75. **Walker, J. E., M. Saraste, M. J. Runswick, and N. J. Gay.** 1982. Distantly related sequences in the alpha- and beta-subunits of ATP synthase, myosin, kinases and other ATP-requiring enzymes and a common nucleotide binding fold. EMBO J. **1:**945–951.
76. **Wang, Z., S. Wei, S. H. Reed, X. Wu, J. Q. Svejstrup, W. J. Feaver, R. D. Kornberg, and E. C. Friedberg.** 1997. The *RAD7*, *RAD16*, and *RAD23* genes of *Saccharomyces cerevisiae*: requirement for transcription-independent nucleotide excision repair in vitro and interactions between the gene products. Mol. Cell. Biol. **17:**635–643.
77. **Yurchenko, V., Z. Xue, and M. Sadofsky.** 2003. The RAG1 N-terminal domain is an E3 ubiquitin ligase. Genes Dev. **17:**581–585.
78. **Zhang, Q., D. Ekhterae, and K. H. Kim.** 1997. Molecular cloning and characterization of P113, a mouse SNF2/SWI2-related transcription factor. Gene **202:**31–37.
79. **Zhang, Z., and A. R. Buchman.** 1997. Identification of a member of a DNA-dependent ATPase family that causes interference with silencing. Mol. Cell. Biol. **17:**5461–5472.
80. **Zheng, N., B. A. Schulman, L. Song, J. J. Miller, P. D. Jeffrey, P. Wang, C. Chu, D. M. Koepp, S. J. Elledge, M. Pagano, R. C. Conaway, J. W. Conaway, J. W. Harper, and N. P. Pavletich.** 2002. Structure of the Cul1-Rbx1-Skp1-F boxSkp2 SCF ubiquitin ligase complex. Nature **416:**703–709.
81. **Zheng, N., P. Wang, P. D. Jeffrey, and N. P. Pavletich.** 2000. Structure of a c-Cbl-UbcH7 complex: RING domain function in ubiquitin-protein ligases. Cell **102:**533–539.